VIRGINIA ELECTRIC AND POWER COMPANY
RICHMOND, VIRGINIA 23261

April 6, 2000

United States Nuclear Regulatory Commission
Attention: Document Control Desk
Washington, D. C. 20555

Serial No.: 00-166A
NL&OS/ETS: R0
Docket No.: 50-338
License No.: NPF-4

Gentlemen:

VIRGINIA ELECTRIC AND POWER COMPANY
NORTH ANNA POWER STATION UNIT 1
ASME SECTION XI RELIEF REQUESTS NDE-9 AND NDE-15

By letter dated March 28, 2000 (Serial No. 00-166), Virginia Electric and Power Company submitted revised relief requests NDE-9 and NDE-15 to address through-wall leakage in the Service Water System as a result of microbiologically-induced corrosion (MIC). Through-wall leakage due to MIC is anticipated to continue to occur during the third ten year ISI inspection interval. The NDE-9 relief request was revised to limit relief applications to socket welds and piping, including butt welds, where flaw characterization cannot be conducted volumetrically or mechanically due to geometry or permanent structural interference. The revised relief request is consistent with Code Case N-513, "Evaluation Criteria for Temporary Acceptance of Flaws in Class 3 Piping," with the following exceptions:

- A through-wall leak may be evaluated or repaired within 14 days.
- Repair or replacement of a through-wall leak may be accomplished within 18 months to coincide with a scheduled service water outage if structural integrity is maintained.
- Results of existing metallurgical analyses may be used to address socket welds and piping, including butt welds, for any location with a through-wall flaw that cannot be characterized volumetrically by ultrasonics (UT) or radiography (RT), or is inaccessible for such treatment.

In a conference call with the NRC staff on April 3, 2000, additional information was discussed relative to Relief Request NDE-9 and the Service Water System MIC issues. The NRC requested that additional information be provided regarding operating experience with MIC in socket welds in the Service Water System. Specifically, the NRC requested destructive examination and evaluation results for the socket welds that have been metallurgically examined. The attachment to this letter provides the information requested by the NRC, including a table of the results of welds experiencing MIC and the examination results, copies of photos of the actual MIC affected areas, and a sketch and associated explanation of our structural analysis methodology for socket welds. In addition, we have provided our basis for addressing butt welds and socket welds collectively due to the similar effect of the corrosion phenomena.

A047

Relief Request NDE-32, which currently provides similar relief, will expire for North Anna Unit 1 at the end of the second ten year ISI inspection interval, i.e., on April 30, 2000. Therefore, NRC approval of Relief Requests NDE-9 and 15 for the third ten year ISI inspection interval is requested prior to that date. Upon expiration of NDE-32 and implementation of NDE-9 and 15, any new through-wall flaws identified in the SW system will be treated in accordance with NDE-9 or 15, as applicable. Previously identified flaws that were assessed in accordance with NDE-32 will not be re-assessed under the new relief requests.

If you have any questions or require additional information, please contact us.

Very truly yours,

David A. Christian
Vice President - Nuclear Operations

Commitments contained in this correspondence: None.

cc: U.S. Nuclear Regulatory Commission
Region II
Atlanta Federal Center
61 Forsyth St., SW, Suite 23T85
Atlanta, Georgia 30303

Mr. M. J. Morgan
NRC Senior Resident Inspector
North Anna Power Station

Mr. M. Grace
Authorized Nuclear Inspector
North Anna Power Station

Attachment

Request for Additional information

ASME Section XI Relief Request NDE-9

North Anna Power Station Unit 1

Virginia Electric and Power Company

Additional Information for Relief Request NDE-9, Revision 1

During a telephone conference with the NRC Staff on April 3, 2000, regarding ASME Section XI Relief Request NDE-9 the following information was requested.

Provide the results of the failure analysis for the flaws associated with MIC in the SW System and a characterization of the flaw

Virginia Power Response:

There have been approximately 102 suspected MIC locations repaired in service water piping since 1996. Forty-five of the locations have been associated with socket welded piping and the balance with butt welded piping. Twenty-six suspected MIC locations have been examined by the failure analysis laboratory. Of these, nine were associated with socket welded piping and 17 with butt welded piping. For five of the socket weld locations, the lab was unable to identify an actual leak location or any evidence of MIC. For the other four, MIC pits with maximum extents ranging from about 0.06 to 0.251 inches were found. In the case of the 17 butt welds, pits with extents ranging from about 0.125 to about 0.562 inches were found. Refer to the Table, "Service Water MIC Pit Sizing," on the next page for details. In addition, although we have not documented in a formal inspection, discussions with inspection personnel indicate that where active leakage was identified, the leak appeared to be in base metal at or near the toe of the weld as opposed to actually penetrating the weld metal itself. Based on the results of failure analysis, MIC attack that results in leakage appears to grow in subsurface extent to no more than about 2.5 times the wall thickness of the affected pipe. Therefore, based on a maximum expected pipe wall thickness of about 0.173 inches (manufacturer's minimum plus 12.5%) for a 2 inch Standard schedule pipe (used in the service water system), it was determined that a 3/4 inch assumed flaw in socket welded pipe would bound any expected degraded condition (Figure 1).

Attached are copies of four failure analysis reports NESML-Q-085, NESML-Q-295, NESML-Q-295A, and NESML-Q-322. These reports depict typical results for failure analysis of piping, which was removed from service because of suspected leakage caused by MIC. In these reports it can be seen that the MIC induced pitting generally begins in the "blued" zone of the base metal contiguous to butt welds or directly under fillet welds. The MIC attack tends to preferentially affect base metal and the heat affected zones of welds, although some attack of weld metal has been noted. Eventual through wall penetration occurs at or near the toe of the associated welds whether it is a butt weld or fillet weld. Figure 1 in the next section depicts the location of the MIC corrosion. In no case was it noted that the MIC attack was associated with any sensitization of weld or base metal. This conclusion is supported by the fact that we have not found excessive ditching of grain boundaries when the austenitic stainless steels are etched with an electrolytic oxalic acid. Based on our failure analysis results and visual inspection of the leakage sites, we have concluded that there is little if any difference in the behavior of the base metals and weld materials relative to weld type, i.e., fillet or butt. Thus, using a 3/4 inch flaw at the weld in conjunction with a straight pipe, as shown in Figure 1, to perform the structural evaluation will adequately establish structural integrity for a flaw detected in the vicinity of a socket weld or butt weld.

North Anna Units 1 and 2 MIC Pit Sizing

Weld ID and/or Line Number	Type	Pit Extent	Wall thickness
2"-WS-777-163-Q3	Socket	0.156	0.187
2"-WS-776-163-Q3	Socket	0.251	0.217
FW 66	Socket	0.06	0.217
FW 67	Socket	None Detected	
FW 73	Socket	None Detected	
FW 74	Socket	None Detected	
FW 90	Socket	None Detected	
FW 96	Socket	None Detected	
4"-WS-46-163-Q3-FW 18W	Butt	0.3	0.216
4"-WS-57-163-Q3-FW 89	Butt	0.3	0.216
4"-WS-46-163-Q3-FW 71	Butt	0.167	0.25
4"-WS-74-163-Q3-FW 9	Butt	0.4	0.233
4"-WS-H84-163-Q3-FW 45	Butt	0.133	0.25
2"-WS-60-163-Q3-FW 58	Butt	0.125	0.188
3"-WS-74-163-Q3-FW 97	Butt	0.125	0.188
2"-WS-84-163-Q23-FW 9W	Socket	0.197	0.154
3"-WS-75-163-Q3-19W	Butt	0.175	0.25
4"-WS-F63-163-Q3-FW 78	Butt	0.375	0.268
4"-WS-57-163-Q3-FW 1W	Butt	0.2	0.25
4"-WS-57-163-Q3-FW 19W	Butt	0.26	0.261
4"-WS-F63-163-Q3-FW 16	Butt	0.24	0.265
4"-WS-F63-163-Q3-FW 13	Butt	0.56	0.26
4"-WS-F63-163-Q3-FW 61	Butt	0.562	0.246
4"-WS-F63-163-Q3-FW 63	Butt	0.2	0.267
4"-WS-F63-163-Q3-FW 64	Butt	0.225	0.249
4"-WS-46-163-Q3-FW 94	Butt	0.36	0.275

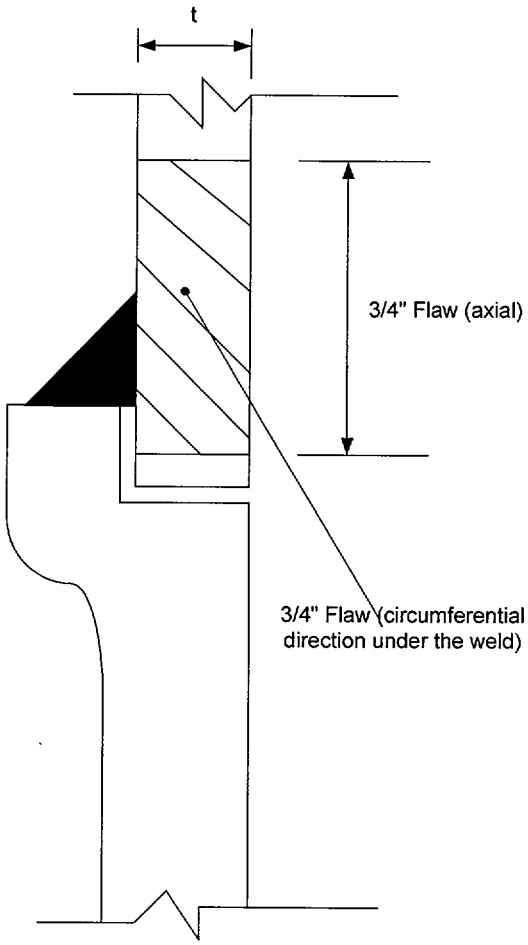

Figure 1
Flaw location

Structural analysis methodology for MIC flaw in vicinity of socket weld.

Virginia Power Response:

Based on the anticipated enveloping flaw on the small-bore (¾"- 2") piping in the vicinity of a fillet weld, the flaw will be modeled for analysis as follows:

i) A ¾ " long through-wall circumferential flaw (Fig 2).
ii) A ¾" long through-wall axial flaw (Fig 3).
iii) A ¾" diameter hole.

The analysis will be performed using the guidance from the ASME Code Case N-513 and ANSI B31.1 Power Piping Code paragraph 104.3. The analysis will treat the flawed location as equivalent to the nominal pipe of the same size containing the enveloping flaw. The required margins in the Code Case will be demonstrated using the loadings due to pressure, deadweight, thermal expansion, seismic OBE and DBE conditions as appropriate. A residual stress equal to the yield stress in the material will be used in the analysis to address the influence of the weld. The ¾" hole will be evaluated using the area replacement method of the ANSI B31.1 Code.

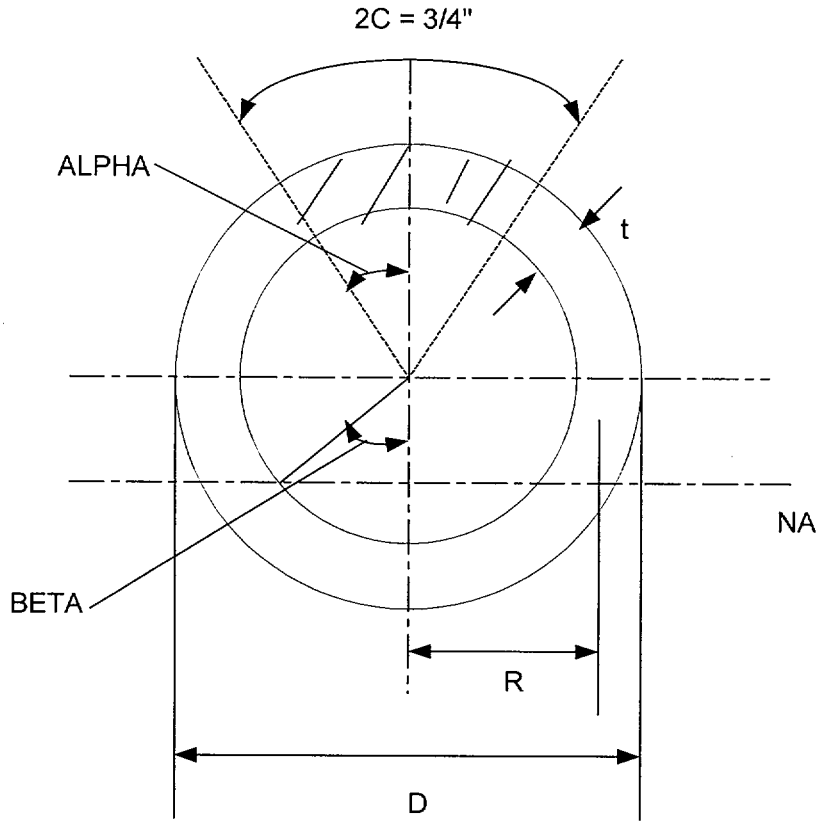

Figure 2
Circumferential Flaw

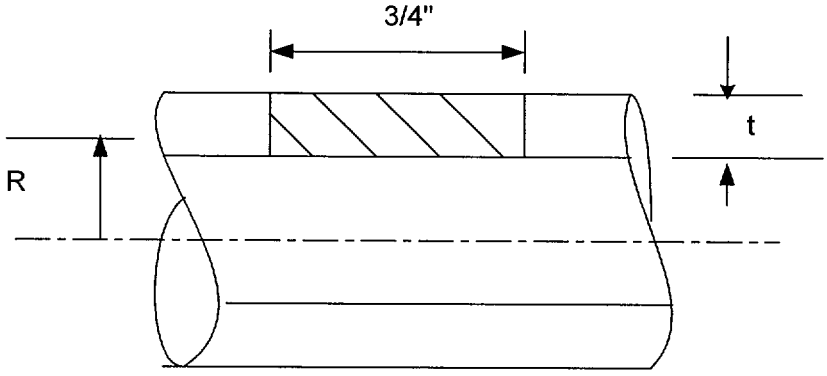

Figure 3
Axial Flaw

DATE: August 6, 1993

NES MATERIALS ENGINEERING LABORATORY
FAILURE ANALYSIS REPORT

NESML-Q-085

1. **Station:** North Anna **2. Unit:** 2

3. **Component:** Line 2"-WS-777-163-Q3, service water discharge from 2-IA-C-1. Socket welded 316L stainless steel schedule 40 pipe.

4. **Safety Related Component:** __X__ **Yes** _____ **No:**

5. **Description of Failure:** A through-wall leak was detected by station personnel in socket weld F-29 adjacent to a 90 degree elbow in the horizontal portion of the 2" pipe run. The line, from the instrument air compressor chiller, had been in service for approximately 2 years.

6. **Laboratory Conclusion:** This failure, which involved 316L stainless steel pipe base metal adjacent to and under several socket weld locations, was a result of microbial influenced corrosion (MIC). Other significant factors were high local strain due to the weld, and oxide tinting on the pipe I.D. surface which also resulted from welding. The rate of pipe wall penetration was relatively fast (2 years), based upon previous experience with stainless steel in the North Anna service water system.

7. **Analyses Performed:** **Results**

Field Inspection: Laboratory personnel inspected the failure location in the North Anna Auxiliary Building basement. The piping run is shown as Figure 1. It was observed that the failure location was in the horizontal orientation adjacent to a reducer at a flow constriction.

Visual Inspection: Visual inspection of the O.D. of the failed socket weld revealed a rust colored region at the area of through-wall penetration shown in Figure 2 as joint "C". Inspection of the I.D. surface under joint "C" revealed a circular region of corrosion products, fairly flat but slightly raised above the pipe surface. This region was surrounded by dark black deposits on the pipe I.D. surface. A similar region of corrosion products was observed at joint "A". Figure 3 shows the deposits at joints "A" and "C". Only black deposits were observed at joints "B" and "D".

Light Microscopy: Light microscopy in the areas of the corrosion buildup revealed corroded and pitted surfaces as shown in Figure 4. Numerous rounded corrosion pits were observed under the corrosion deposits. The pitting was highly localized to an area approximately 1/2" in diameter in joints "A" and "C" of Figure 2. Only light corrosion damage was seen at joint "B". All corrosion pitting was observed to have initiated on the 316L pipe I.D. surface in the region of oxide tinting (Figure 5) under, or adjacent to, the socket weld in a region showing high local strain.

Metallography: Metallography through joints "A" and "C" revealed corrosion pitting expanding from small entrance holes on the pipe I.D. surface under, or adjacent to, the socket welds, Figure 6. Metallography of the pipe base metal just below the weld showed a shallow region of melting and recrystallization. The major portion of the base metal below the weld, and at the pipe I.D. surface, showed no sign of melting ("melt-through") during the welding process. Corrosion pitting initiated in unmelted base metal below, or adjacent to the socket weld location in the region of the oxide tinting from welding. Corrosion progressed into weld metal only after penetration of base metal in the weld area. Weld metal corrosion, therefore, was not a significant factor.

EDS Analysis: EDS semi-quantitative chemical analysis of the corrosion products revealed green deposits rich in Cr, brown deposits rich in Fe, and black deposits very rich in Mn with P and S. Other elements such as Si, Ca and Mg were found which indicate mud or silt from the reservoir liner. This grouping of elements is typical of corrosion products and deposits associated with MIC. Table 1 presents these results.

Quantitative Chemistry: Quantitative chemical analyses were made, by an outside test lab, of the fitting, weld metal, and pipe at the through-wall penetration of joint "C". These analyses are presented as Attachment 1, and they show all materials to be 316L stainless steel with a carbon content of 0.02 percent. These are acceptable results for the "L" grade material.

Oxalic Acid Etch Test: An ASTM A262 Practice A oxalic acid etch test was conducted on metallographic cross sections of the corroded socket weld. The etch test revealed that there was no sensitization of the 316L base metal under the weld metal. This finding was as expected.

Microbiological Analysis: A microbiological analysis (Attachment 2) was conducted by BTI, for Virginia Power, of corrosion products from the I.D. surface of joint "C" near the through-wall penetration. BTI noted that there were high levels of total bacteria and SRB. It was further noted that the diverse bacterial community was composed primarily of bacilli (rod-shaped bacteria), with sub-populations of

spherical bacteria, and filaments and sheaths. Filaments and sheaths are unusual morphological features and serve as presumptive evidence for metal oxidizing and depositing capabilities.

Local Strain Measurements: Diameter reduction measurements were made on joints received into the laboratory, and joints in the field in line 2"-WS-777-163-Q3. It was determined that at weld toe regions, on the pipe O.D., deformation across the diameter was on average 0.004" on one axis and 0.006" on the other axis. This represents a significant strain, with residual stress levels at yield strength values. When joints were cut in the laboratory, diameters tended to further reduce, due to high circumferential stress.

8. **Comments:** There were several significant factors in the corrosion related failure of the 2" diameter 316L S/S socket weld in 2"-WS-777-163-Q3 in a period of approximately 2 years. These were:

   A. A diverse bacterial community with very high levels of metal oxidizing and depositing bacteria and SRB. This community appeared to produce a local environment particularly destructive to the protective film on 316 stainless steel.

   B. Zones of mud or silt, which combined in low levels with the bacterial community, to produce a cover deposit over the stainless steel surface. Stainless steel becomes more sensitive to corrosion damage as the surface becomes locally covered, preventing a uniform contact with oxygen to replenish the protective film.

   C. Strain from welding in the 316L pipe base metal under the socket weld. Corrosion sensitivity is known to be influenced by high local strain. This may be a result of formation of cathodic and anodic regions.

   D. Oxide tinting under the socket weld and on the I.D. surface of the 316L pipe. The Nickel Development Institute (Tuthill and Avery, 1992) notes that "Removal of the heat tint may be necessary to prevent corrosion in acidic environments". The Cr rich region of the corroded surface of the 316L stainless steel pipe clearly indicates that the pipe was locally exposed to an acidic MIC environment. Such an environment would not normally be expected in the service water system at North Anna Power Station, and thus no requirement existed to prevent (or remove) the oxide tint. The oxide tint could have been prevented by use of an inert gas purge at welding. The tint also could be removed by in-situ pickling. Pickling with a HNO_3-HF bath is usually only accomplished

at a mill or fabrication facility, and is not normally a field option.

E. The horizontal orientation of the joint in combination with the close proximity of a reducer. These factors, combined with the slight diametrical constriction resulted in an ideal region for accumulation of deposits.

F. The warmer water associated with the discharge region of the heat exchanger. Microbial/bacterial growth is often accelerated by warmer water conditions.

While all of the above factors are significant in the corrosion damage of the pipe, it must be stressed that the most significant factor is the particular bacterial community found at this location. An analysis of one other stainless steel failure in the NAPS service water system (in 1992) revealed a similar total microbial count and microbial community. However, the high levels of Mn found in the present failure were absent, but chloride was present in that failure as well as higher levels of Al and Si. In the 1992 failure, acid producing (APB) bacteria were detected in high levels as well as SRB. In the present failure, SRB was detected in slightly higher levels, as well as higher levels of metal oxidizing and depositing bacteria. There was less mud or silt in the present failure as compared to the 1992 failure. This indicates that throughout the NAPS service water system we may find similar bacterial communities, but there also may be differences accounting for locally more, or less, corrosive conditions. The oxide tinted location appears to have been the least corrosion resistant, and the attack occurred at this location.

9. **Recommendations:** The failure and deep pitting, in two years of operation, of the socket welds in line 2"-WS-777-163-Q3 demonstrates the extreme sensitivity of 300 series stainless steel to some forms of MIC attack. This is the first time we have clearly documented rapid failure of 316 or 304 stainless steel, in the North Anna service water system by microbial attack. This failure suggests that we consider a program to define the extent of the current problem and provide a resolution. The laboratory considers that the following actions would be consistent with a definition/resolution of this type of problem:

A. Define the "high damage potential" locations for stainless steel pipe in the NAPS service water system based on failure location reports, and an inspection program designed to reveal such areas. This inspection program would employ radiography at selected locations, as well as engineering analysis/selection of higher temperature low flow regions. Areas of flow constriction, horizontal pipe locations, discharge sides

of heat exchangers and regions where deposits accumulate should be considered.

B. Halt any further "general" change-out of service water lines to 304 or 316 stainless steel. It seems likely that the 300 series of stainless steels does not possess the corrosion resistance to resist some forms of microbial attack now occurring in the NAPS service water system at "high damage potential" locations. However, at many locations within the system this material seems to perform quite well, and might continue to be the material of choice.

C. Evaluate the use of other replacement alloys such as AL6X and Inconel 625 for certain "high damage potential" locations in the NAPS service water system.

D. Monitor the bacterial levels in the service water system, especially at "low-flow" or "occasional-flow" stainless steel lines.

E. Determine whether "low-flow" or "occasional-flow" lines should/could be operated differently, to achieve more consistent flow.

F. Define ways to make the biocide treatment program more effective. This may involve use of cleaning agents in water treatment for stainless steel lines, and concurrently addressing the clay liner issue which would certainly now prevent the use of cleaning agents (dispersants).

G. Perform an engineering evaluation to determine the extent of circumferential damage which might be tolerated in the stainless steel lines prior to structural collapse. At present, the small through-wall pits in this line probably do not present any structural problem. This type of damage, however, may spread around the circumference and weaken the ductile austenitic pipe material to a point where the line could fail by plastic hinge (collapse).

Prepared By: J. M. McAvoy

Checked By: J. G. Beck

Attachments

JMM/pg

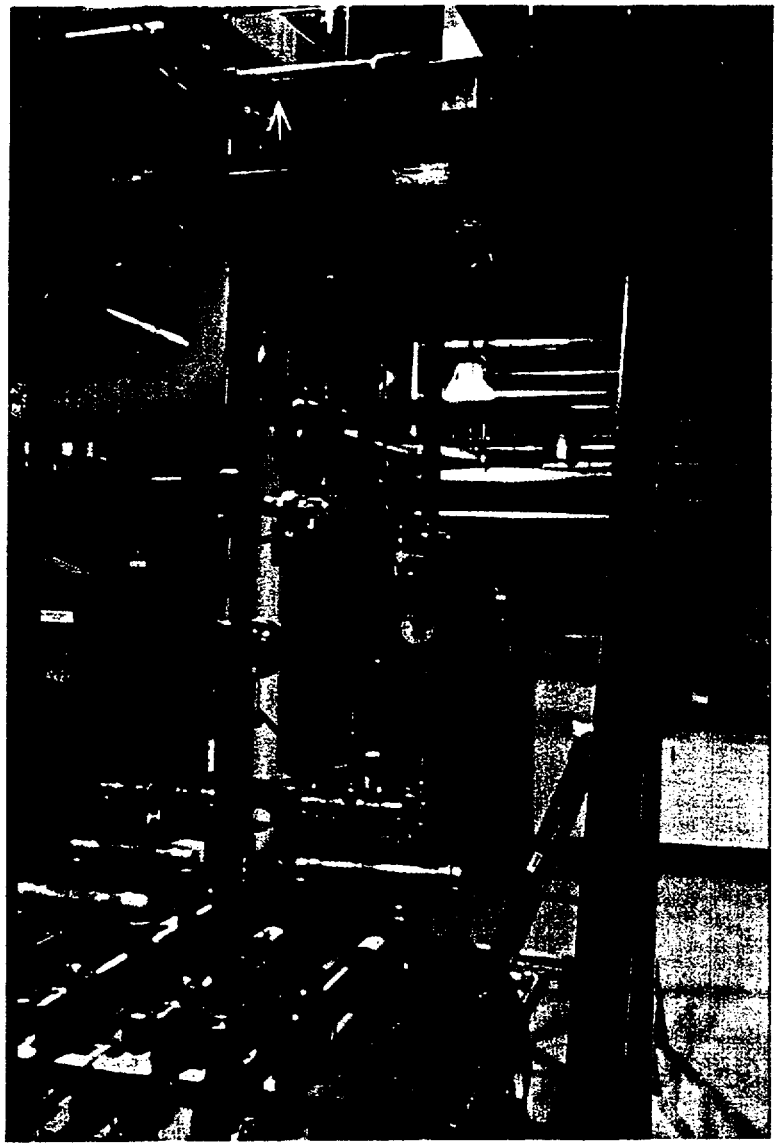

Figure 1: Line 2"-WS-777-163-Q3 with arrow indicating failure location in the horizontal elbow socket weld.

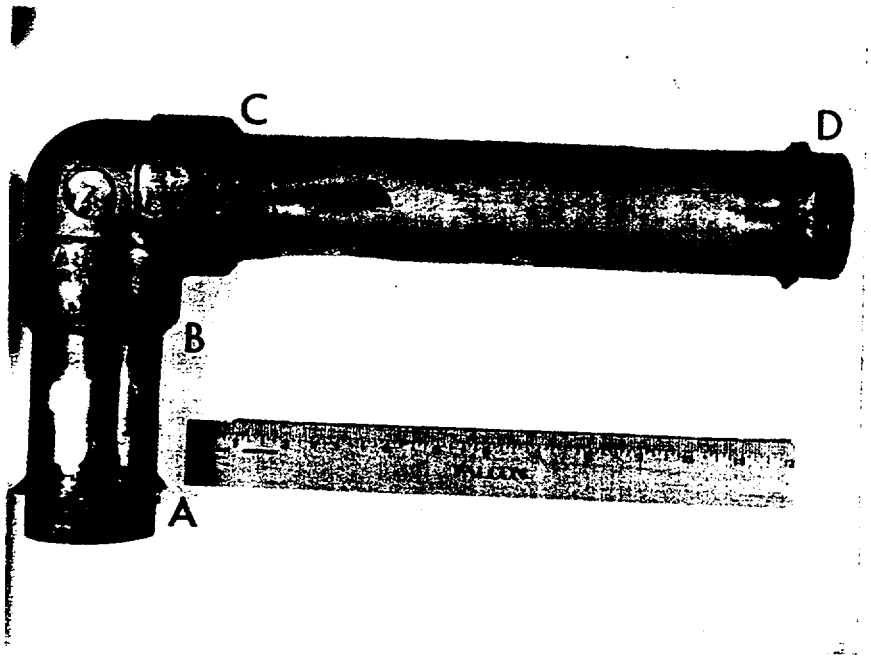

Figure 2: Through-wall leak location ("C") in elbow socket weld in line 2"-WS-777-163-Q3. Deeply pitted region was observed at location "A", and incipient corrosion pitting at "B".

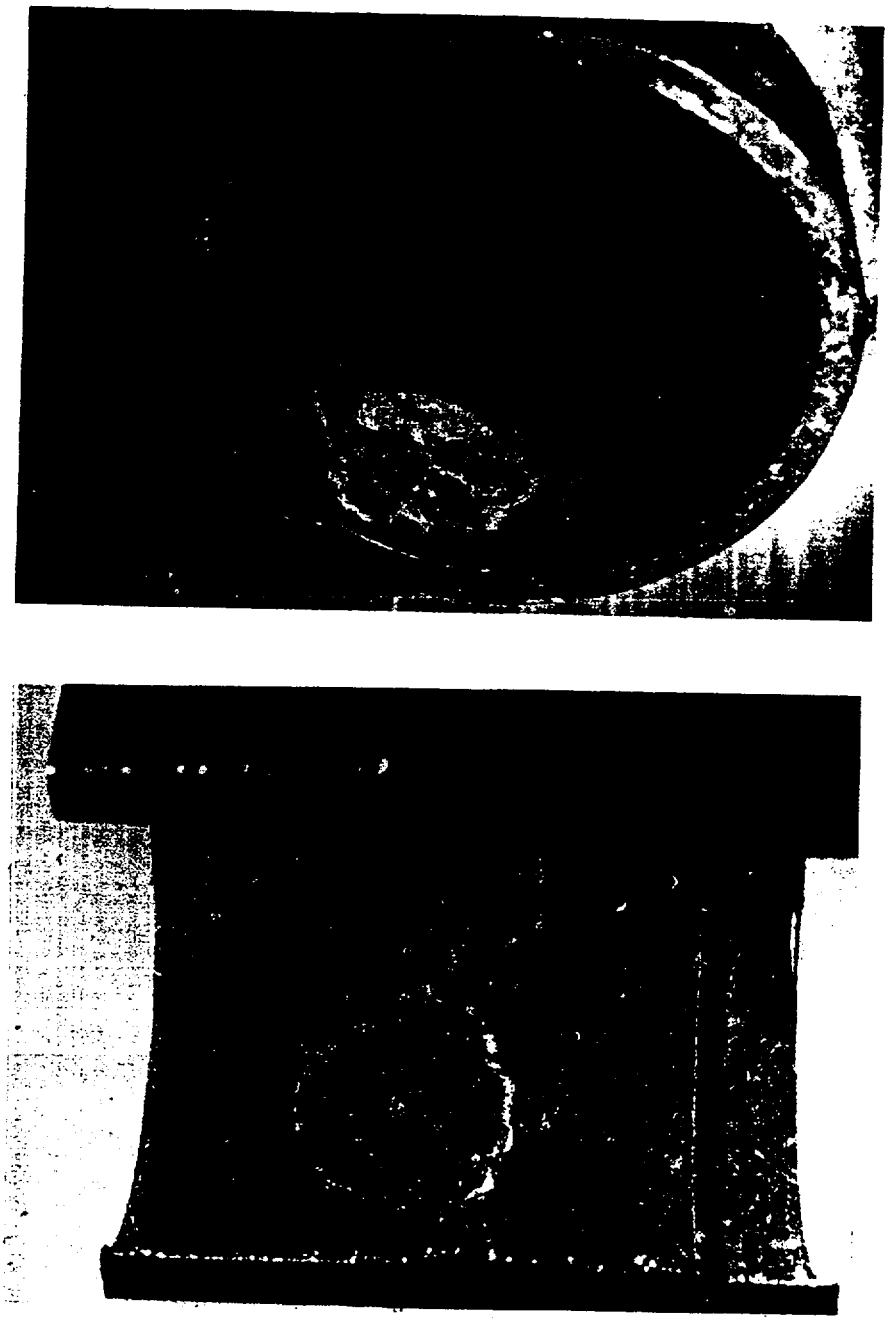

Figure 3: A (above), corrosion products/deposits observed at area "A" of Figure 2. Corrosion pitting approximately 85% through-wall was observed under this deposit. B (below), corrosion products/deposits observed at area "C" of Figure 2. This was the through-wall MIC pit.

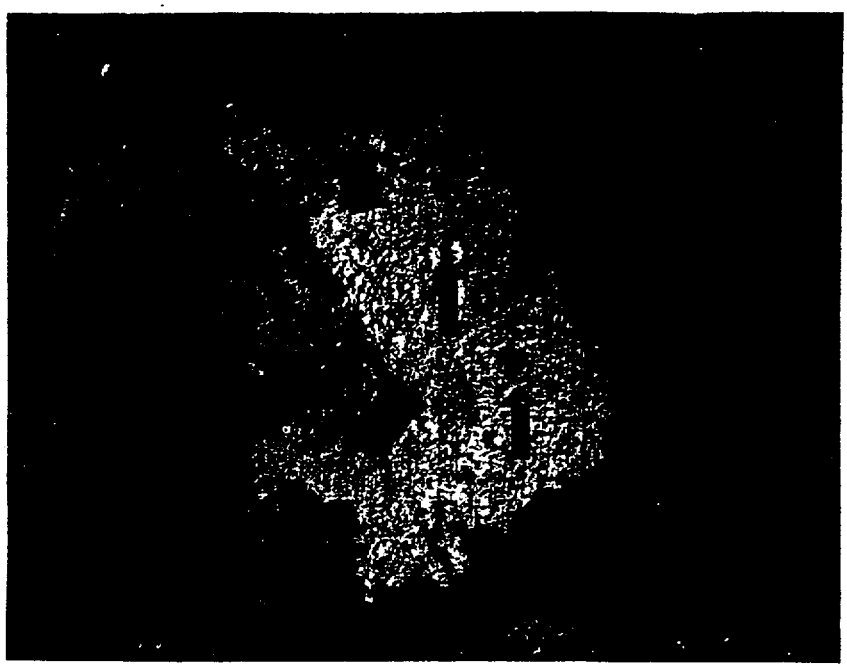

A

B

Figure 4: A (above), appearance of corrosion pitted region of pipe under socket weld at area "A" of Figure 2, showing deep "MIC" corrosion pits (arrows). Magnification 4.5X. B (below), appearance of corrosion pitted region of pipe under socket weld at area "B" of Figure 2, showing only incipient corrosion damage (arrow). Magnification 3.5X.

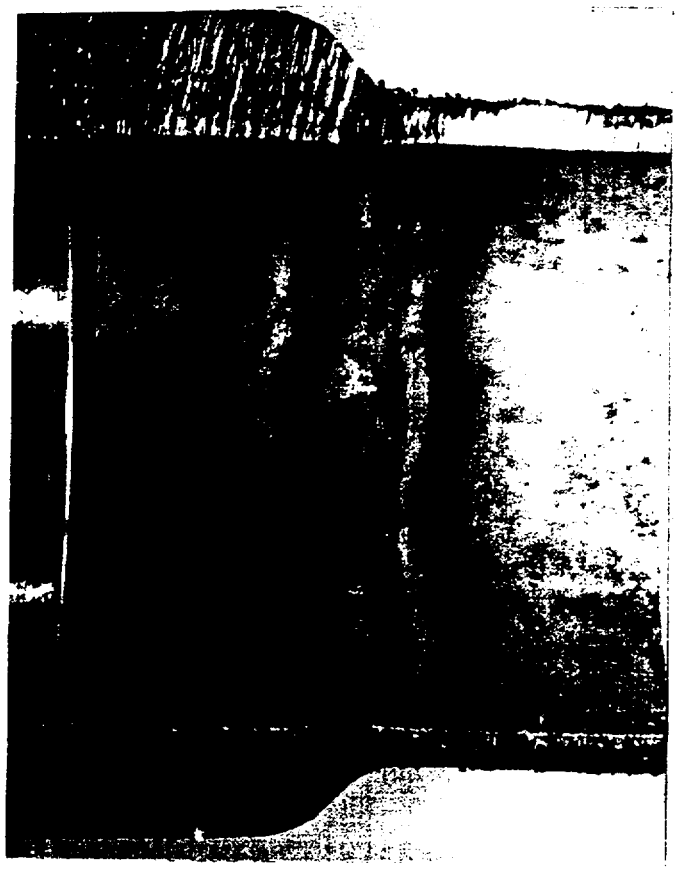

Figure 5: General appearance of oxide tinted region below the socket weld of location "C" of Figure 2, at an area 90 degrees away from the corrosion damaged area (at top). Magnification ≈1.5X.

A

B

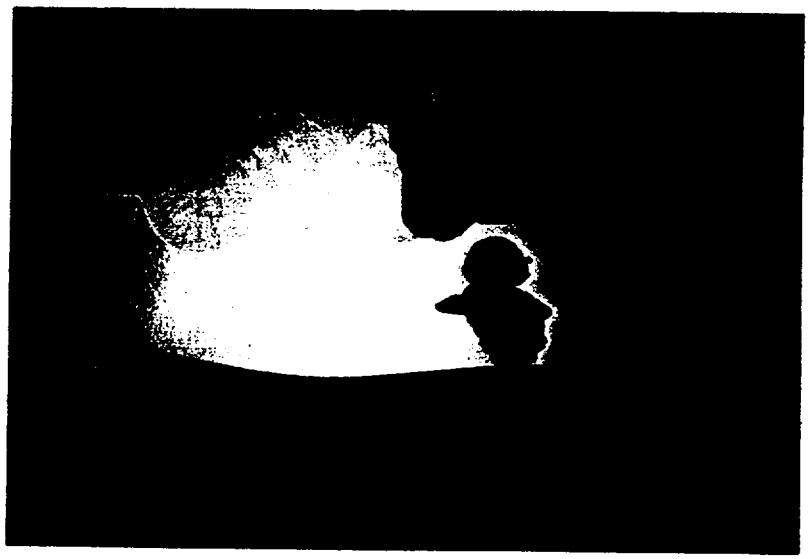

C

Figure 6: A and B (above) right side and left side of a single cut location through the corroded area of location "C" of Figure 2. This is the through-wall location at the toe of the socket weld. The corrosion pit initiates at the I.D. surface (A) and grows circumferentially to the O.D. surface (B). C (below), shows the 85% through-wall corrosion pit at location "A" of Figure 2. This pit initiated behind the socket weld in the pipe stub end. All magnifications 4X. Oxalic acid etch.

TABLE 1

Semi-Quantitative EDS Results
NAPS S/S SW Pipe Failure
Line 2"-WS-777-163-Q3

	WEIGHT %														
SAMPLE	Fe	Cr	Mn	Ni	S	Mo	Si	P	Ca	Zn	Mg	Ti	K	Na	O*
Pipe Base Metal	66.09	18.37	1.96	12.10		1.47									
Elbow (Socket) Base Metal	67.28	16.86	1.74	11.43		2.24	0.39								
Weld Metal	64.55	18.83	1.72	11.95		2.09	0.72								
#1 Yellow Deposit	68.44	0.50	1.77	2.05	0.00	5.04	4.79	6.65	5.23	2.03	3.50				
#2 Green Deposit	22.70	50.27		1.37	0.40	17.56	3.09		4.62						
#3 Small Particle (Wide Shot)	48.93	16.11	2.18		0.00	23.26	4.60	1.69	3.23						
#3A Dark Particle	11.07	1.16	31.06		0.75	10.66	19.84	5.35	8.32	4.05	3.92	0.62	1.13	2.08	
#3B Charging Particle	9.08	52.59		0.50	0.00	28.54	3.30	0.73	5.26						
#4 Small Particles (Wide Shot)	52.87	14.76	2.62	1.40	0.54	20.93	3.94	0.64	2.82						
#4A Charging Particles	36.73	24.77		1.08	0.09	28.95	4.21	0.68	3.50						
#5 Black Deposit	48.74	1.51	20.61		1.61	3.37	7.89	4.73	7.57	3.54		0.44			
#6 Light Brown Deposit	70.41	0.75		2.03	0.50	21.81	2.48	0.49	1.53						
#7A Small Black Flecks	10.60		42.83		0.87	4.35	21.83	3.46	8.77	5.00		1.48	0.81	0.00	
#7B On Pipe I.D.			55.80		0.94	4.81	11.74	3.29	9.06	6.02	7.07	0.96	0.32	0.00	
#7C Not at Failure	7.27	0.69	61.23		1.33	1.97	9.75	1.88	7.70	6.90		1.05	0.22		
	Fe	Cr	Mn	Ni	S	Mo	Si	P	Ca	Zn	Mg	Ti	K	Na	O*

* Small Oxygen Peak Present On Each Sample.

ATTACHMENT 1

NNI Chemical Analysis

Newport News Industrial Corporation

700 Thimble Shoals Blvd.
Suite 113
Newport News, Virginia 23606-2544
804-380-7053

Subsidiary of
Newport News Shipbuilding
A Tenneco Company

July 12, 1993

Virginia Power Company
ISI/NDE and Engineering Services - I
5000 Dominion Boulevard
Glen Allen, Virginia 23060

Attention: Mr. Joe McAvoy

Subject: Chemical Analysis

References:
(a) Your Purchase Order BST 423109, Release 8
(b) Our Job Order 2351-L-45008

Enclosure:
(1) Test Report - NNS Lab. Number 93008193

Gentlemen:

Enclosure (1) is forwarded and is the result of tests performed in accordance with References (a) and (b).

We look forward to serving you in the future. Thank you.

Very truly yours,

T. E. Bond
Manager Industrial Products

/llf

NNS LABORATORY SERVICES, 031,1 07/08/93 15:29

FINAL

LAB NUMBER : 93008193 DATE ENTERED : 07/07/93 COMPLETED : 07/08/93 15:22
REQUESTOR : LAURA DEPT. : NNI CHARGE : 5176L45008
PO.OR.NO. : BST R423109 R8 ITEM : NNPN :
DWG/GRP/SH/LINE : JOB ORDER 2351L45008
MATERIAL : 316L STAINLESS STEEL
SYS/ART/LOC : 2" SOCKET WELD FROM NORTH ANNA S.W. PIPE
SPECIFICATION : AISI 316L?
PURPOSE OF TEST : INFORMATION: 3-CHEM, 1-FITTING, 1-WELD, 1-PIPE
HEAT NO.: LOT#: LOT SIZE: SAMPLE SIZE: 1
CONTROL LEVEL : QID TAG NO. : 053 CNTL# OR 195# : V875571
MANUF/CUST : VIRGINIA POWER/INNSBROOK
COMMENTS(1) : SEE ATTACHED SKETCH FOR LOCATION OF ANALYSES
COMMENTS(2) : FAX TO LAURA @ 83841 WHEN COMPLETE
COMMENTS(3) : JHA
DISTRIBUTION(1) : 3-LAURA-NNI-PICKUP BASKET

PARAMETER	RESULT
(CHEMICAL ANALYSIS OF FERROUS BASE METALS)	
CHROME (%)	16.05
MANGANESE (%)	1.52
NICKEL (%)	12.23
MOLYBDENUM (%)	2.19
COPPER (%)	.04
SILICON (%)	.34
TITANIUM (%)	N.A.
VANADIUM (%)	N.A.
ALUMINUM (%)	N.A.
PHOSPHORUS (%)	.013
SULPHUR (%)	.008
CARBON (%)	.02✓
LEAD (%)	N.A.
ZIRCONIUM (%)	N.A.
COBALT (%)	<.01
COLUMBIUM (%)	N.A.
TANTALUM (%)	N.A.
BORON (%)	N.A.
REMARKS	FITTING
ANALYST(S)	HR
SAMPLE NO.	1
(CHEMICAL ANALYSIS OF FERROUS BASE METALS)	
CHROME (%)	17.04
MANGANESE (%)	1.44
NICKEL (%)	13.45
MOLYBDENUM (%)	2.30
COPPER (%)	.10
SILICON (%)	.40
TITANIUM (%)	N.A.
VANADIUM (%)	N.A.
ALUMINUM (%)	N.A.
PHOSPHORUS (%)	.027
SULPHUR (%)	.010

ATTACHMENT 2

BTI Report

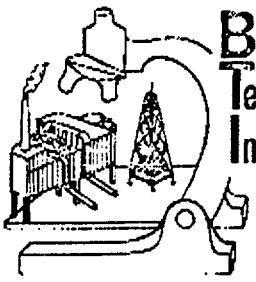

Bioindustrial
Technologies
Incorporated

Specialists in
Microbial Detection
and Control

P.O. Box 323
Grafton, N.Y. 12082
(518) 279-9731

FACSIMILE TRANSMISSION

July 7, 1993

Virginia Power
ISI/NDE & Engineering Svcs - I
Mr. Joseph McAvoy
5000 Dominion Blvd.
Glen Allen, VA 23060

Dear Mr. McAvoy:

Included in this transmission please find one *draft* copy of our final report on the microscopic analysis of a corrosion product sample.

Please telephone (**1-800-323-9731**) at your earliest convenience with any questions, comments, edits, etc. so we can incorporate them and forward the final hard copy to you. If we do not hear from you within 5 working days from the date of this fax we will assume our report is satisfactory and we will automatically mail you a hard copy.

Thank you for your continued interest in BTI.

Sincerely,

Todd M. Kenney
Biologist

David M. Dziewulski, Ph.D
Dir., NY Office

TK:lvh
transmission
photocopy: client file

MICROSCOPIC ANALYSIS OF A CORROSION PRODUCT SAMPLE

Submitted to

VIRGINIA POWER
Glen Allen, VA

By

BIOINDUSTRIAL TECHNOLOGIES, INC.
Grafton, New York

Bioindustrial™ Technologies Incorporated

July 7, 1993

INTRODUCTION

One corrosion product sample was collected by Virginia Power (VP) personnel from a service water system pipe. The dry sample was shipped from VP and received at the Bioindustrial Technologies, Inc. (BTI) laboratory in Grafton, NY on 7/2/93. The sample was assigned the following BTI control number:

BTI#	Sample Description
930316	Service Water Pipe Deposits (2"-WS-777-163-Q3)

Mr. Joe McAvoy of VP requested that the following microbiological analyses be performed on the sample: (1) total bacterial count using epifluorescence microscopy, (2) sulfate-reducing bacteria (SRB) count using indirect fluorescent antibody analysis and (3) microscopic detection of any metal-depositing bacteria (e.g., iron- and manganese-depositing bacteria). Please refer to appendix A for detailed materials and methods.

RESULTS

Table 1. Results of Microscopic Analysis			
Sample	Total Direct Bacterial Count, FITC Method♦	Sulfate-Reducing Bacteria Count, SRB-IFA Method♦	Comments
930316 Corrosion product (cells/g)	1.3×10^9	7.3×10^6	Diverse community composed primarily of rod-shaped bacteria, with subpopulations of cocci (spherical bacteria) and filaments (some with sheaths and deposits)
♦ See Appendix A for details of FITC and SRB-IFA			

COMMENTS

Direct epifluorescent microscopic examination of the sample revealed high levels of total bacteria and SRB. The diverse bacterial community was composed primarily of bacilli (rod-shaped bacteria), with subpopulations of cocci (spherical bacteria) and filaments (some with sheaths, and others with associated deposits).

Filaments with sheaths (and/or associated metal deposits) are unusual morphological features characteristic of certain groups of bacteria. These characteristics serve as presumptive evidence for metal-oxidizing and -depositing capabilities. However, it should be noted that many bacteria which are capable of depositing metals do not have any unusual morphological characteristics which would separate them from other bacterial groups. Positive identification of the latter organisms requires culture methods that are difficult and time consuming.

In addition, flocs of FITC-reactive material containing cells and particulates were seen in the sample. The FITC-reactive material was most likely exopolysaccharide (EPS, or slime) of microbiological origin.

APPENDIX A: MIC ANALYTICAL MATERIALS AND METHODS

Liquid Samples. The various analytical methods described below were performed directly on raw water samples. No sample manipulation was necessary to prepare liquid samples for these analyses. Levels of microorganisms and chemical analytes were reported on a per milliliter basis for liquid samples.

Solid Samples. In order to analyze solid samples using the following analytical methods, it was first necessary to convert the samples to aqueous slurry form. This was accomplished by adding a known amount of raw solid sample to a given volume of sterile deionized water. The mixture was then thoroughly homogenized to form a uniform suspension. This slurry was then used to perform a dry weight determination as well as the various analytical techniques. Since the amount of solid material in the slurry was known, levels of microorganisms and chemical analytes were converted and reported on a per dry gram basis.

Semi-solid Samples or Liquid Samples with Associated Solids. Samples that are neither truly liquid or solid were analyzed as liquid samples, if possible. If samples of this nature could not be handled as a liquid, then a dry weight determination was performed and levels of microorganisms and chemical analytes were converted and reported on a per dry gram basis.

Dry Weight Analysis. In order to determine the levels of microorganisms and soluble chemical analytes per unit dry weight of solid or semi-solid samples, a total residual weight was performed on the raw samples or sample slurries. This was accomplished by weighing a given amount of sample, completely drying the sample at 105°C, and re-weighing it. (APHA Standard Methods 17th ed., [1989]).

Viable Bacterial Counts. BTI MICKIT™ media were used to determine the levels of viable bacteria belonging to one or more of the following four categories: (1) Acid-producing bacteria (APB, which are facultative and/or obligate anaerobes capable of producing organic acids), (2) sulfate-reducing bacteria (SRB, which are obligate anaerobes capable of reducing sulfate to sulfide), (3) aerobes and (4) obligate or facultative anaerobes. This method employs serial dilution to an end-point extinction to estimate the numbers of viable bacteria to the nearest order of magnitude

INT Viability. Samples were processed, as soon as possible after collection, for viable counts using the INT method as follows: Approximately 40 ml of each sample was placed in a sterile 50-ml centrifuge tube. The samples were then incubated for one hour with p-iodonitrotetrazolium violet (INT) and respiratory substrates. The INT dye precipitates (as a formazan crystal) intracellularly within actively respiring cells. The INT reaction provides an estimate of the percentage of the microbial population that is viable. Following the incubation period, the samples were treated with a 37% solution of formaldehyde (final concentration of formaldehyde was 3.7% v/v) in order to kill and preserve the microbial populations present in the sample for microscopic examination. These were subsequently viewed using epifluorescence and bright-field microscopy (see below).

Epifluorescence, Bright-Field, and Phase-Contrast Microscopy. A portion of the samples and dilutions were spotted, dried and heat-fixed to multi-well slides, and stained with fluorescein isothiocyanate (FITC). The total microbial populations (both live and dead) were then enumerated using epifluorescent microscopy. For those samples which had previously been INT reacted, random fields were re-read using phase-contrast microscopy in order to determine the INT viability of the populations. In addition, combined epifluorescence and phase-contrast microscopy were used to detect bacteria, with unusual morphologies, which have been implicated in MIC (e.g. the iron oxidizing and depositing bacteria Gallionella, Hyphomicrobium and related bacteria) It should be noted that not all bacteria capable of oxidizing metals will have unusual morphologies. If requested, samples were also prepared for indirect fluorescent antibody analysis for sulfate reducing bacteria (SRB-IFA). Such immunofluorescence microscopic techniques are useful for determining the presence of specific organisms when viable culture analysis is no longer a reliable method of detection (e.g. for samples which have been dried and/or exposed to air). It should be stressed, however, that these methods detect live or dead, culturable or non-culturable bacteria.

Anion Analysis. A portion of the samples were filtered through a 0.2 micron (nominal pore size) syringe filter directly into a sealed nitrogen-filled bottle. Ion chromatography analysis of the soluble anions in the filtrates was performed at the BTI laboratory using a Dionex 2000i/SP ion chromatograph with a Dionex 4270 integrator. The column used was a Dionex AS4A Ion Pac^{R}column with a flow rate of 2.0 ml/min. The column eluate was 1.8 mM Na_2CO_3/1.7 mM $NaHCO_3$. The regenerant used was 0.025 N H_2SO_4. Component identification by the integrator was made by comparison to pre-run standards used to make a three point linear calibration based on three different concentrations of the anion standard stock solution containing 0.1, 1.0, and 10.0 ppm each of sodium chloride, sodium nitrite, sodium nitrate, potassium phosphate and potassium sulfate (APHA Standard Methods 17th ed., [1989]).

Organic Acid Analysis. A portion of the samples were filtered through a 0.2 micron (nominal pore size) syringe filter directly into a sealed nitrogen-filled bottle. A portion of the filtrates were then acidified and the organic acids were extracted into an organic solvent. Complete partitioning was performed by freezing. The organic portion was then decanted into a vessel containing anhydrous sodium sulfate to remove any traces of water. The samples were then analyzed by gas chromatography using a packed column and a water/oxygen free helium carrier. Concentrations were determined by comparison to pre-run standards. Monitoring routinely involves the detection of the following organic acids: formic, acetic, propionic, isobutyric, butyric, isovaleric, valeric, isocaproic, caproic and heptanoic. The detection limit for this test (low-end sensitivity) is 2.0 ppm.

Metals Analysis. A portion of the samples were filtered through a 0.2 micron (nominal pore size) syringe filter directly into a sealed nitrogen-filled bottle. A portion of the filtrates were then digested with nitric acid. The acidified sample solution was heated until clear and no visible particulates remained or until the volume was reduced by 50%. Digested samples were then analyzed for the specific metal(s) requested by the client. All analyses were conducted via atomic absorption spectroscopy on a Perkin-Elmer AA Spectrophotometer, Model 5100 equipped with an HGA-600, graphite furnace and Zeeman background collection.

Total Volatile Solids. In order to get an estimate for the levels of organic carbon in the samples, total volatile solids (TVS) were determined by drying a known volume of sample at 105°C, weighing, then igniting the dried sample at 550°C, re-weighing, and determining the amount of weight lost on ignition (APHA Standard Methods 17th ed., 2540 B & E, [1989]).

NES MATERIALS ENGINEERING LABORATORY
FAILURE ANALYSIS REPORT
January 28, 1997

NESML-Q-295

1. **Station:** North Anna Power Station 2. **Unit**: 1&2

3. **Sample Origin:** Service water piping from lines 4"-WS-46-163-Q3, 4"-WS-56-163-Q3, 2"-WS-60-163-Q3, and 3"-WS-74-163-Q3.

4. **Safety Classification:** SR

5. **Description of Failure:** At least four locations in the above listed service water piping were observed to have developed through wall leaks in, or adjacent to, the field welds. Pipe sections containing the leak locations and adjacent welds were removed and submitted to the ITC Materials Laboratory for examination.

6. **Laboratory Conclusions:** The through wall leaks that occurred in the service water piping resulted from pitting which initiated and propagated due to microbiologically influenced corrosion (MIC). There were fourteen other welds associated with the removed lines that were inspected in the lab. All of the welds appeared to show some evidence of microbiological activity. The degree of damage varied considerably, ranging from only one or two small nodules along the ID, accompanied by little or no damage to the underlying metal, to several large nodules under which there was pitting almost completely through wall. The quality of several of the welds examined was marginal, in that there was evidence of slag inclusions, uneven penetration, and areas of melt through. Some of these imperfections resulted in discontinuities along the ID surfaces of the welds and apparently provided locations that were ideal for the onset of microbiological activity.

7. **Discussion:**

Visual Inspection, Light Microscopy and Metallography: A total of eighteen welds were inspected in the laboratory. Roughly half of the welds showed only minor damage in the form of one or two small nodules with little or no accompanying surface damage. Even on those welds that exhibited the most extensive damage in the form of large nodules and deep, or in some cases through wall pits, the damage was not wide spread around the circumference of the weld. There appeared to be no well defined linear arrangement of the pits along the weld surface. Instead, in situations where there was more than one area of pitting, the damage seemed to be randomly spaced around the circumference.

A summary of the results obtained from visual, light microscopy, and metallographic inspection for the most heavily damaged welds is provided below.

4"-WS-46-163-Q3-18W: The segment of pipe that was submitted to the lab containing this weld is shown in *Figure 1*. The initial inspection of the ID surface revealed approximately seven nodules along the circumference of the weld. Six were small to medium in size but the remaining nodule was fairly large. *Figure 2* shows the large nodule along the ID surface of the weld after the pipe was sectioned in half. Evident in the photo is a circular area of discoloration next to the large nodule that may have been the location of another large nodule that had been dislodged. Cleaning of the surface and microscopic inspection revealed that two of the smaller nodules were actually areas of weld metal melt through that had become covered with deposit. The weld contained several pits, some of which were in the center of the weld, *Figure 3*, while others were closer to the edge of the weld near the heat affected zone (HAZ), as shown in *Figure 4*. A metallographic cross section was prepared on the pit shown in *Figure 4*. The results are presented in the two views shown in *Figure 5*. The top photo shows the damage as it first appeared upon inspection, approximately 1/3 of the way through the weld. The bottom photo shows how the pit expanded and branched out towards the pipe base metal. This subsurface branching was observed in several of the pits and is a classic indicator of MIC damage.

4"-WS-57-163-Q3-FW89: The section of pipe submitted to the lab containing this weld is shown in *Figure 6*. There was evidence of staining along the OD of the pipe to indicate that there was leakage occurring at this location. This weld joined two 90° elbows and therefore the ID could not be visually examined without sectioning the pipe. Inspection of the pipe after sectioning revealed only one moderately large nodule along the weld, as shown in *Figure 7*, which corresponded to the location on the OD staining. Microscopic inspection of the ID surface of the weld after cleaning revealed no evidence of any major corrosion damage. The only area that appeared to show any damage was a lightly etched area In the center of the weld. This area, when touched with a spatula, was extremely soft, and further probing resulted in a hole appearing in the center of the weld as shown in *Figure 8*. There were at least two other welds that showed a similar pattern of damage, in that no evidence of ID pitting was present, other than a light area of etched metal which eventually opened into a pit. Metallographic examination of this area revealed a pit that started near the center of the weld and progressed through the weld in a more diagonal path towards the HAZ and base metal of the pipe as shown in *Figures 9* and *10*.

4" WS-46-163-Q3-FW71: The section of pipe submitted to the lab for examination containing this weld is shown in *Figure 11*. The ID surface contained only one moderately large nodule, located on base metal but encroaching on the ID weld toe. Removal of the nodule and deposits revealed a fairly large pit, approximately 1/8 inch in diameter, approximately 1/4 inch from the weld, as presented in *Figure 12*. Metallographic inspection of this weld again showed evidence of classic microbial damage. *Figure 13* contains the two photomicrographs taken from the prepared cross section. The presence of two separate pits that eventually join, is again an indication of branching of the corrosion pits.

3"-WS-74-163-Q3-FW9W: The section of pipe submitted to the lab for analysis that contained this weld is shown in *Figure 14*. This section of pipe displayed evidence of staining on the OD indicating an apparent through wall leak at the weld. The ID surface showed the remnants of three nodules, one appeared to be large and corresponded with the apparent leak location on the OD. The other two appeared to be moderately sized. All three were located on the weld as shown in *Figure 15*. Cleaning of the pipe surface revealed a very rough and irregular weld profile, making it difficult to determine if pits and cavities present under the removed nodules, displayed in *Figure 16*, were related to MIC or the welding operation. Two areas thought to be small nodule-like areas were actually determined, after cleaning, to be areas of weld melt through. A metallographic cross section was prepared through the weld in the area shown in *Figure 16* which corresponded to the area under the largest nodule. This section revealed corrosion damage that was not only similar to the damage at several of the other welds but was again a classic example of microbiologically influenced corrosion attack. *Figure 17* is a photographic montage showing the corrosion pit at this weld. The pit appears to have propagated along the weld/base metal interface, and to have undergone extensive lateral expansion (roughly ½ inch in total length) into the pipe wall.

4"-WS-H48-163-Q3-FW45: * This particular weld was selected for examination because, unlike the previous welds examined which were stainless steel welds, this weld was made using a high nickel (Inconel) filler metal. The section of pipe containing this weld is shown in *Figure 18*. This weld also showed evidence of leakage on the OD of the pipe. Inspection of the ID surface revealed only staining where one medium sized nodule had apparently previously existed as displayed in *Figure 19*. At this location there were three to four small pits that can be seen in the slightly higher magnification views contained in *Figure 20*. The pitting was approximately 1/4 inch from the weld into the pipe. A metallographic section taken through this area revealed the pitting to be approximately 1/3 of the way through the pipe wall, as shown in *Figure 21,* and not affecting base metal.

* - During removal of the pipe section in the field, the pipe was cut through the field weld identification number marking on the pipe making positive identification of the weld impossible.

2"-WS-60-163-Q3-FW58: This weld was submitted to the laboratory for examination because an excessive number of indications were detected during radiographic inspection. The weld was part of the reducer shown in the photograph labeled *Figure 22*. Evidence of nodules from microbial activity can be seen along the ID in *Figure 23*. The weld profile from the ID can be seen in *Figure 24*. The appearance of the weld was extremely rough and irregular, with evidence of excessive melt through and incomplete fusion along the surface. The surface of the weld was cleaned and then sectioned approximately every 1/8 inch for roughly 1/2 the circumference of the pipe as shown in *Figure 25*. The results

revealed large amounts of slag inclusions throughout the weld and cracking in some areas. Several of these areas can be seen in *Figure 26.*

Although there was apparent MIC activity occurring along the weld, most of the NDE concerns related to this weld appear to be the result of poor workmanship during fabrication of the joint.

3"-WS-74-163-Q3-FW97: This was another weld which, like FW58 above, exhibited extensive evidence of MIC attack as judged from X-rays. The weld between an elbow and what was a vertical run of piping is shown in *Figure 27.* Two close up views of the weld from opposite sides of the pipe are shown in *Figure 28.* From these it can be seen that the quality of the final pass of the weld varies significantly around the circumference of the pipe. *Figure 29* shows the condition of the root of the weld in two half sections of the circumference before removal of the corrosion product, while *Figure 30* shows the sections after cleaning. In these views it can be seen that the weld root pass was in poor condition with evidence of melt through, suck-up, lack of penetration, and possible sugaring. Some of the pitting caused by the MIC attack is also evident in the view of sample "B", at the arrows.

In an effort to assess the extent and seriousness of the MIC attack and possible weld discontinuities, sample "B" of FW97 was sectioned similar to FW58 with the difference that in this case the weld was sectioned by grinding about every two millimeters in a plane parallel to the toes of the weld. The resulting sections revealed that the weld actually exhibited little or no internal weld defect but did show extensive evidence of MIC attack. The MIC attack was mostly discreet indications. The attack was concentrated near the center of the weld appearing to initiate in the root pass discontinuities and the HAZ. The sizes of the individual areas of attack ranged up to about 6 millimeters in any direction with an average size of about 4 millimeters and a generally spherical shape. *Figure 31* shows three of the progressively ground sections spanning the center of the weld and the predominant damage.

EDS Analysis: Energy dispersive spectroscopy (EDS) was utilized to determine the elemental compositions of some of the deposits and nodules that were removed from the ID surfaces of several of the welds. The significant findings that would indicate microbial activity in the damaged areas were as follows:

1) Areas of manganese-rich deposit and scale were found. The high levels of this element most likely indicates the presence of manganese-reducing bacteria.

2) The detection of large amounts of chromium in the corrosion products. This can sometimes suggest extremely acidic conditions within the corrosion cell. The high chromium levels can also suggest the presence of bacteria that can

metabolize chromium.

3) High levels of sulfur were detected in the corrosion products. Large amounts of sulfur usually indicate that sulfate reducing bacteria (SRB) were involved in the corrosion process.

Typical spectrum printouts showing each of the three areas discussed is included in *Figure 32.*

EDS was also used to verify the alloy compositions of all of the welds listed above. The welds, with the exception of FW-45, were specified to be 300 series stainless material (308 s/s). The spectrums obtained from these welds were appropriate for the type of material. As previously stated, field weld 45 was reported to be a high nickel-base alloy (Inconel). The spectrum obtained from this sample was also appropriate for that material. All of the pipe was labeled 316 stainless and was verified by EDS.

8. Conclusions: The cause of leakage from the stainless steel service water piping seen in the lab to date has been microbiologically influenced corrosion. This is based on visual and microscopic examinations of the pipe surfaces and chemical analyses of the corrosion deposit and ID scale. The corrosion resulted in at least four through wall pits at, or adjacent to, the stainless steel welds. Often this attack seems to have its initiation at weld root discontinuities. Besides the failure locations, fourteen other welds were examined in the lab. All of them showed evidence of microbiological activity. In general, the MIC attack involves one or two localized indications along the pipe weld. Most of the damage was rather minor, consisting of only a few small pitted areas around the weld. There were several areas, however, where the damage was more widespread, resulting in a greater number of pits along the weld that were much larger in size due to extensive subsurface branching. The only weld that did not display any corrosion damage was field weld 45, which was a high nickel alloy weld. Nevertheless, even at this location, there was MIC damage adjacent to the weld in the pipe base metal.

Several of the welds were of poor quality, resulting in very rough and porous root profiles. Notable among these were 3"-WS-74-163-Q3-FW97 and 2"-WS-60-163-Q3-FW58. While not totally responsible for the corrosion damage, these geometric discontinuities undoubtedly played a role in the establishment of the microbial colonies. In conjunction with the failure analysis effort for those two welds, and several others, the lab has had the opportunity to compare weld X-rays, X-ray interpreter reader sheets, and actual weld conditions as determined by metallographic sectioning. In those cases where large amounts of nearly continuous MIC attack are noted on the reader sheets (FW97 and FW 58), examination of the welds has found significant weld quality problems, as discussed previously and also including some lack of fusion, along with the MIC attack that was noted. Examination of the X-rays revealed that in those cases where MIC attack is

superimposed on poor quality welds it can be difficult to reliably differentiate one from the other. Sectioning of these two welds revealed that the degradation of weld metal cross sectional area was probably less severe than suggested by the X-rays. From a intuitive and non-analytical perspective it did not appear that the welds would be significantly structurally challenged by the conditions noted. In those cases where only a few widely scattered MIC indications are seen on the X-rays, the reader sheets and actual weld conditions compare favorably. These conditions also appear much easier to assess structurally than those with much MIC and poor weld quality.

Recommendations: At present it is difficult to accurately characterize welds with significant pre-existing weld root quality anomalies and MIC attack together, making it likely that these welds will have to be repaired when found. It may be helpful to continue to remove such welds when discovered by X-ray and evaluate them in the Materials lab to attempt to establish a better correlation between the appearance of the X-rays and the actual weld discontinuities.

Prepared by: 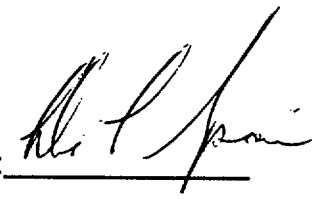

Reviewed by: 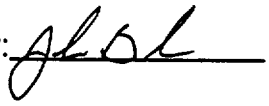

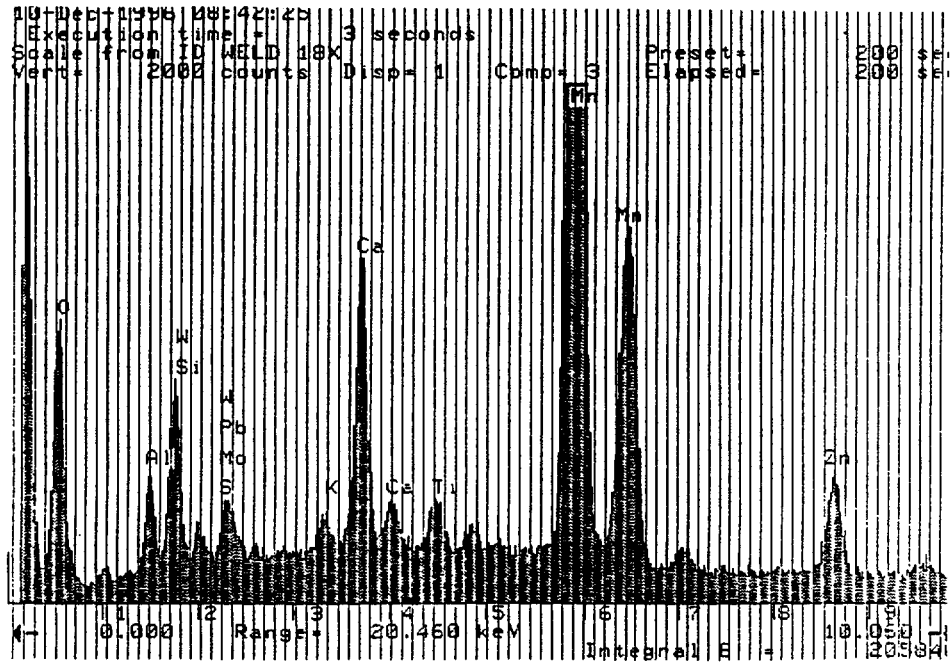

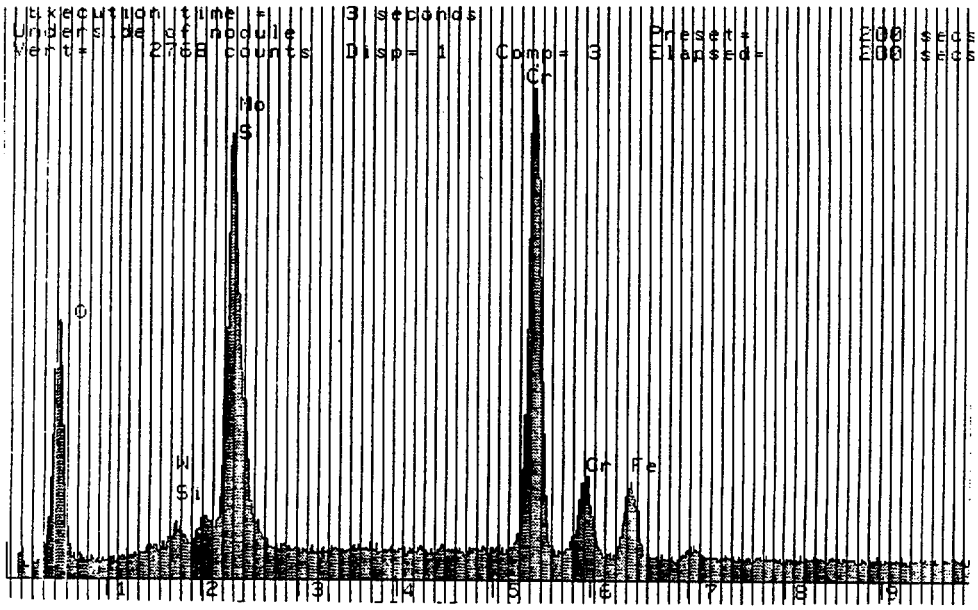

Figure 32: EDS spectrum printouts showing the areas of high manganese (top scan), chromium, and sulfur (bottom scan).

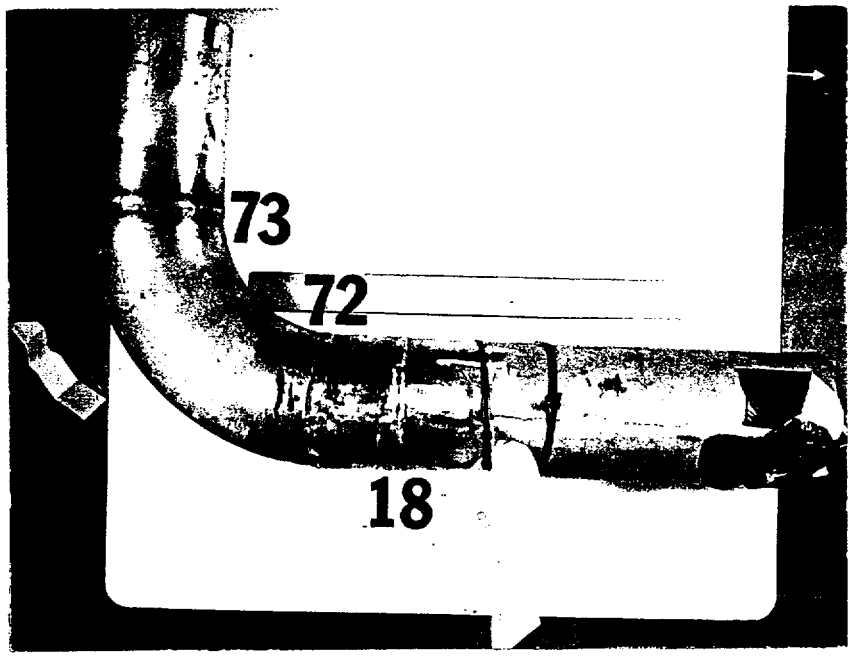

Figure 1: Photograph showing the segment of pipe containing field weld 18W.

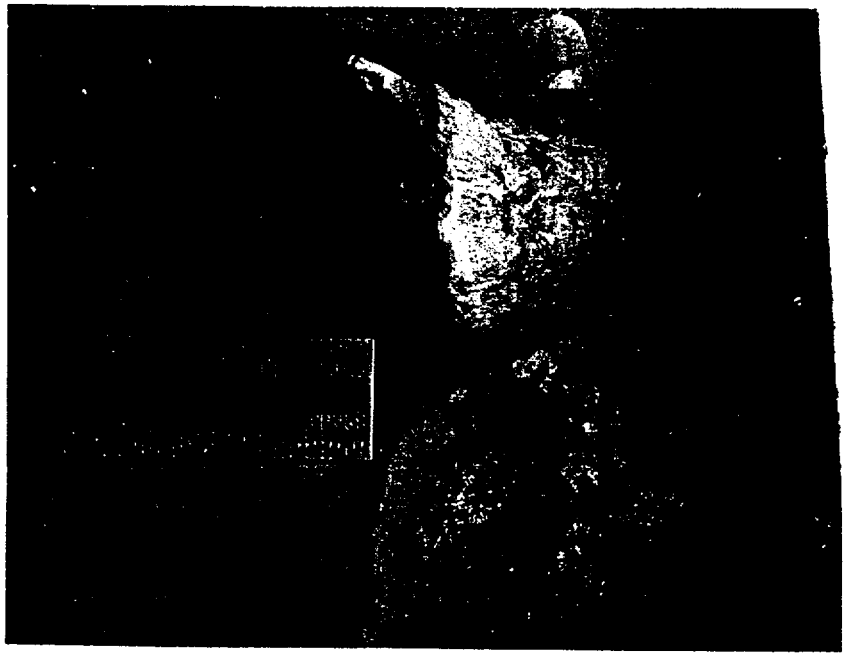

Figure 2: View of the ID surface of the pipe at weld 18W after sectioning into two halves, showing the large nodule present along the weld. The orange-yellow staining near the nodule may have been the previous location of another nodule.

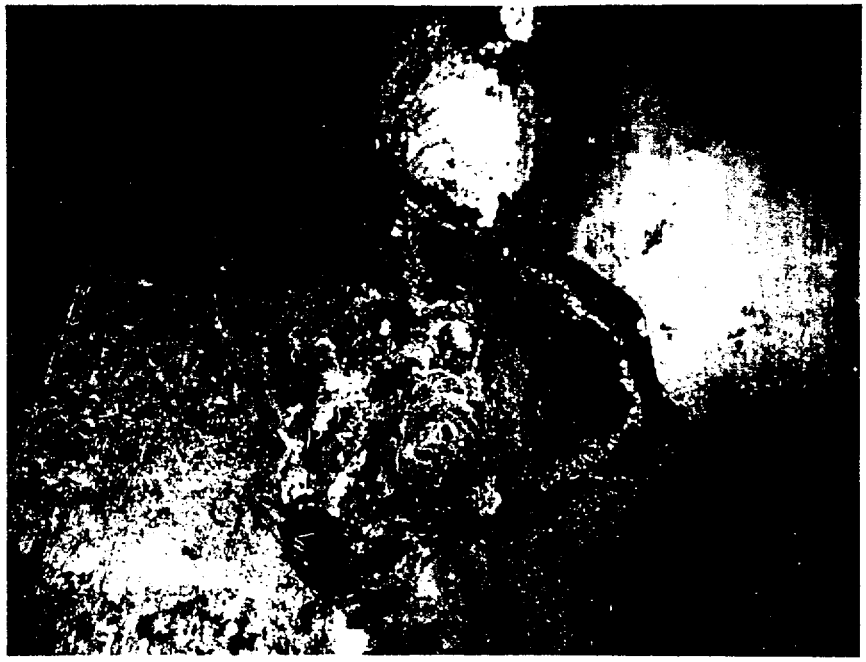

Figure 3: Photograph of the ID surface after cleaning, showing some of the pitting that was present under one of the nodules along weld 18W. Mag. 6X.

Figure 4: View of more pitting along the ID of weld 18W. Mag. 7X.

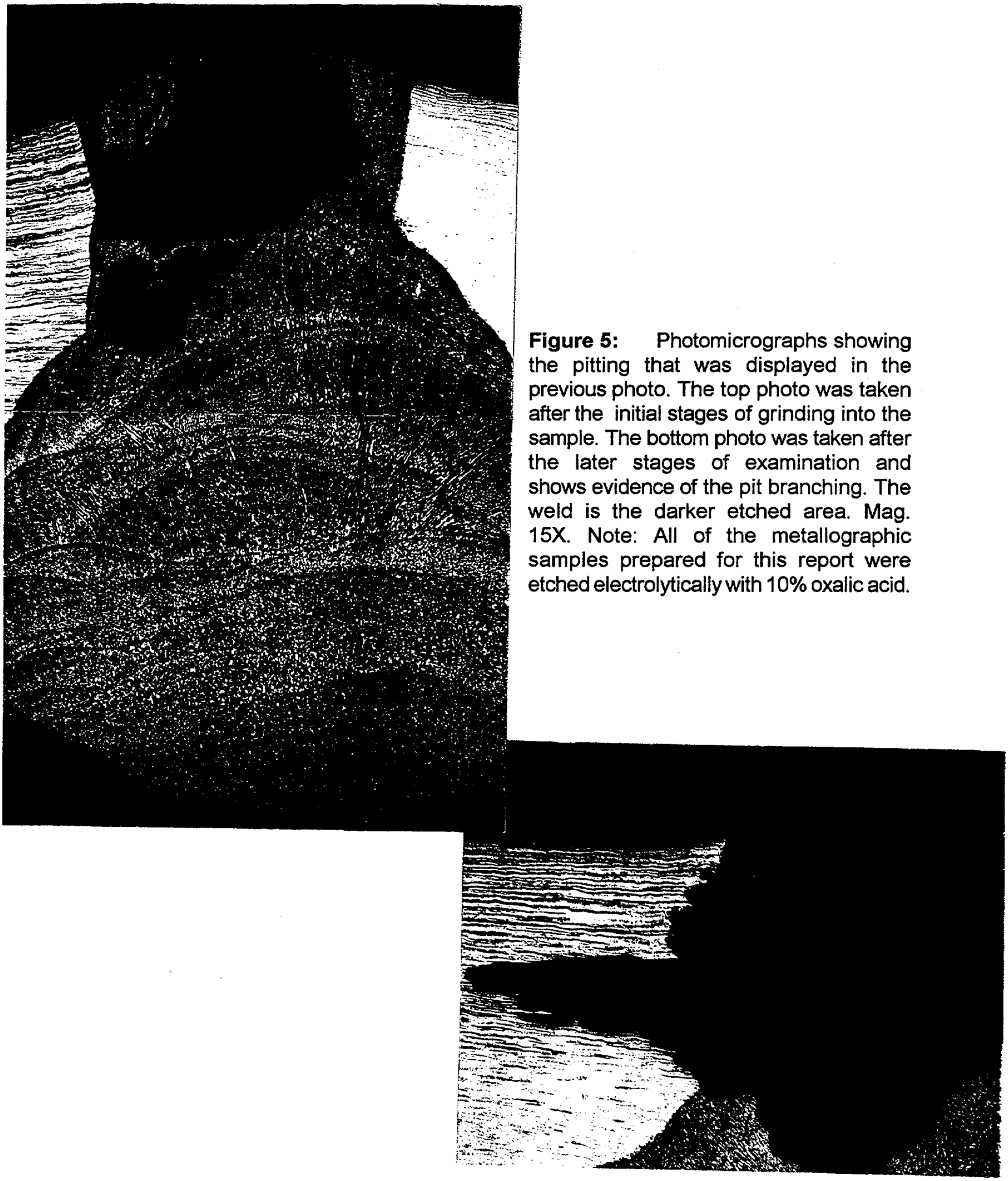

Figure 5: Photomicrographs showing the pitting that was displayed in the previous photo. The top photo was taken after the initial stages of grinding into the sample. The bottom photo was taken after the later stages of examination and shows evidence of the pit branching. The weld is the darker etched area. Mag. 15X. Note: All of the metallographic samples prepared for this report were etched electrolytically with 10% oxalic acid.

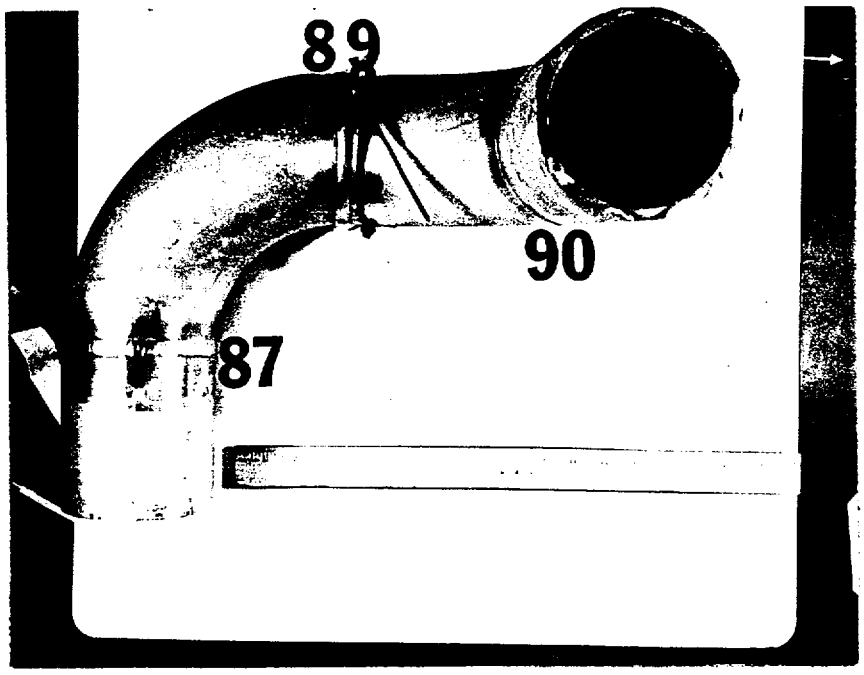

Figure 6: Photograph showing the section of pipe containing field weld 89.

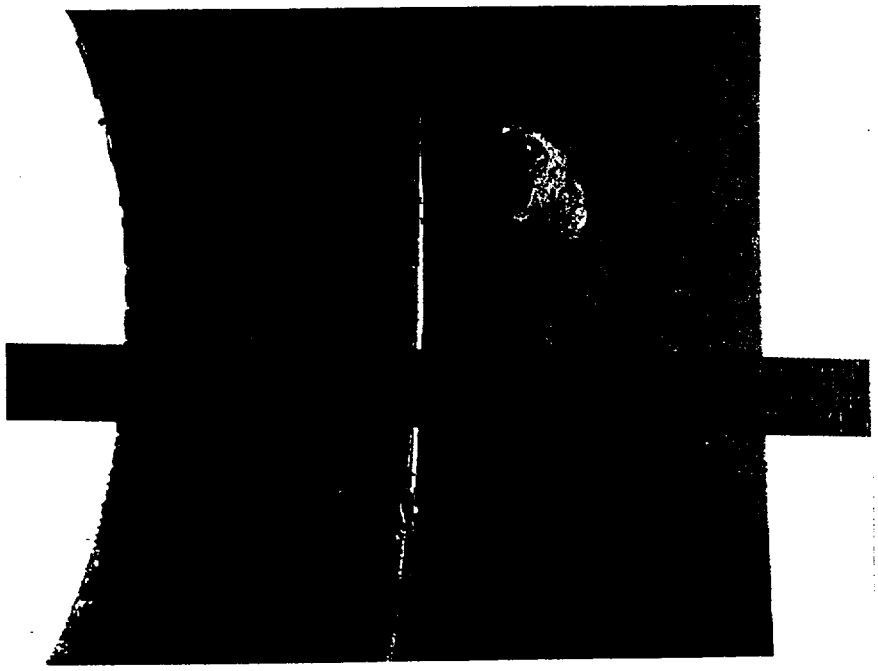

Figure 7: View of the ID surface of weld 89 showing the corrosion nodule present.

Figure 8: Closeup view of the center of weld 89 and the small hole (arrow) that was made in the laboratory by touching the weld with a spatula. Mag. 7X.

Figure 9: Photomicrograph showing the pit in the previous photo as it was first detected during metallographic examination. Mag. 15X.

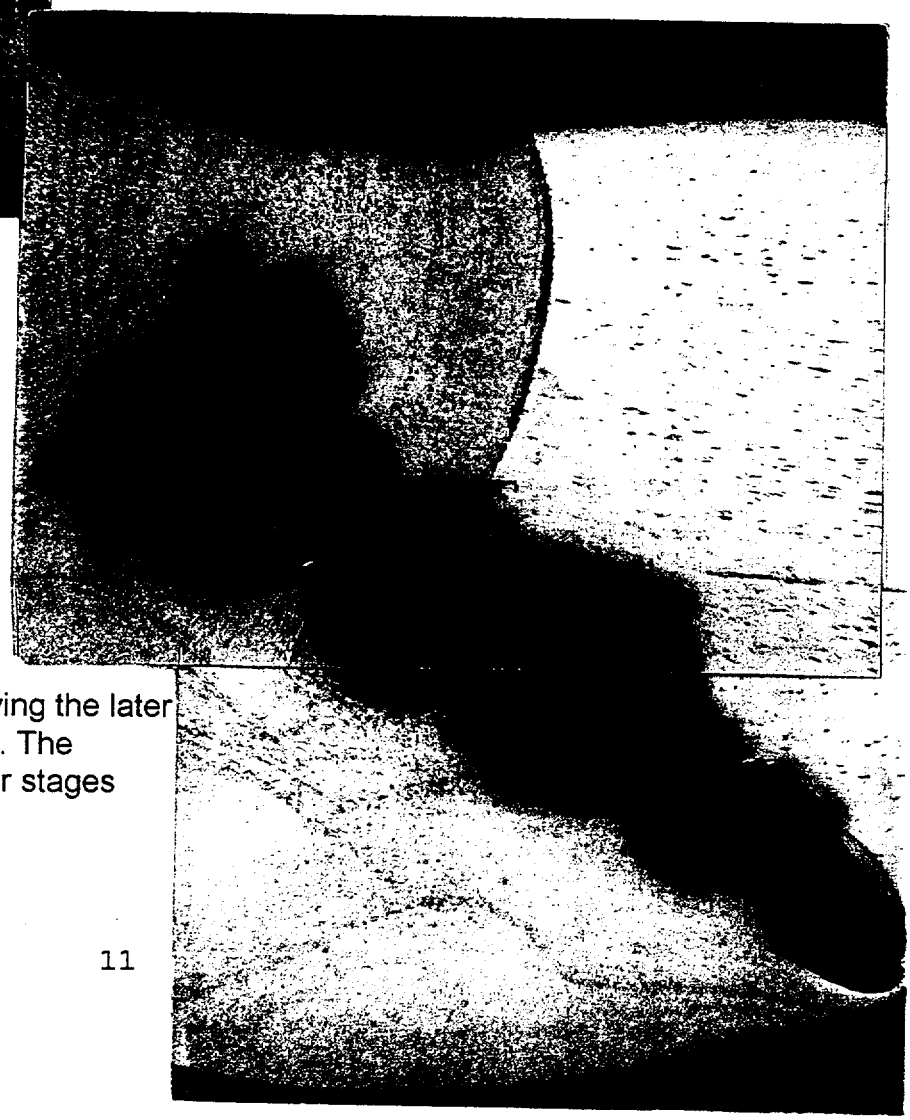

Figure 10: Photomicrograph showing the later stages of metallographic inspection. The lateral extension of the pit in its later stages is clearly evident. Mag. 15X.

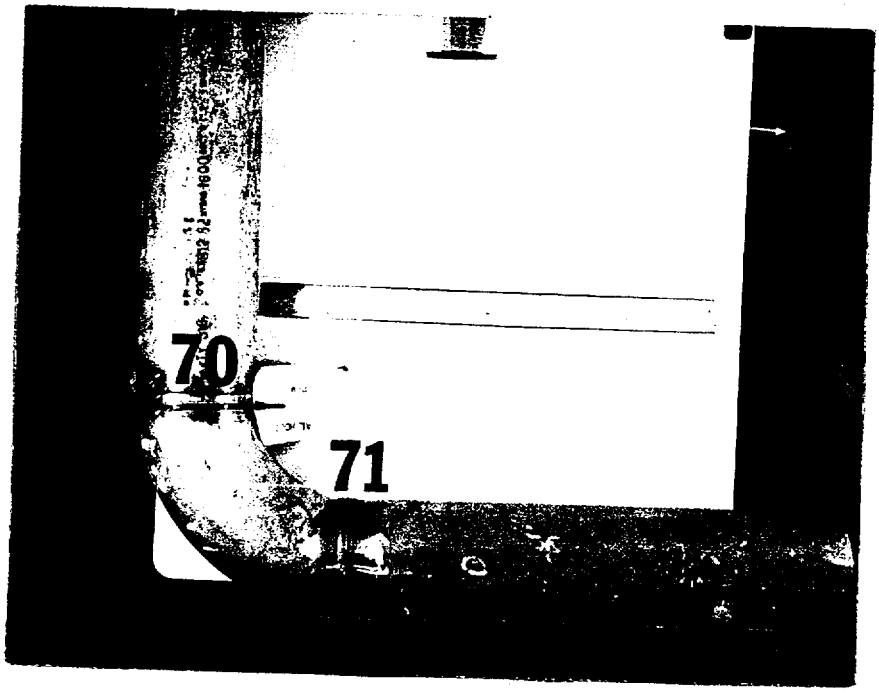

Figure 11: Photograph of the section of pipe containing field weld 71.

Figure 12: Photograph of the pit that was present under the large tubercle on the surface of the weld 71. Mag. 7X.

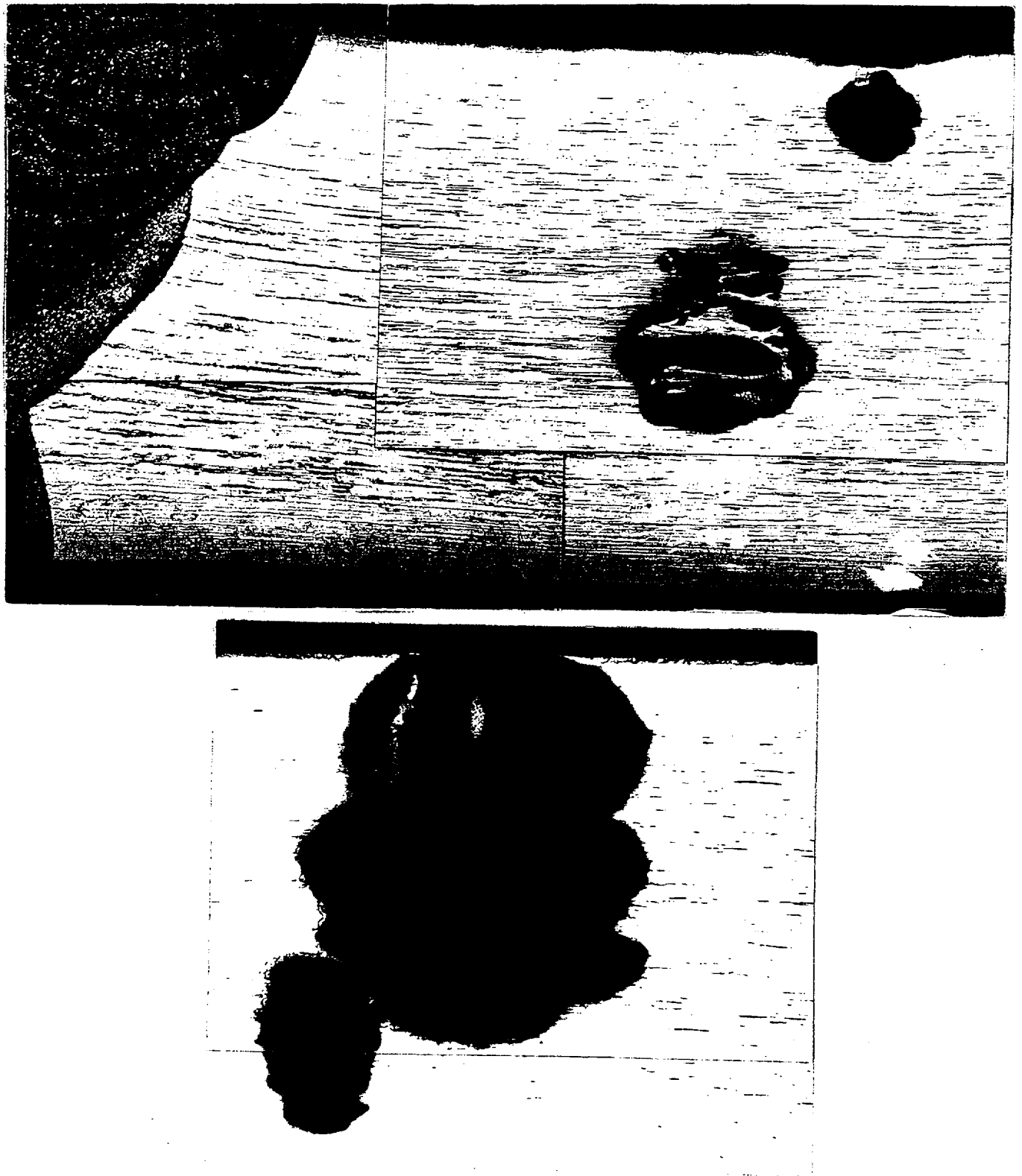

Figure 13: Photomicrographs taken from the metallographic sample prepared through the pit shown in the previous figure. The top photo was taken upon initial discovery of the pitting. The appearance of two pits in the photo indicates branching of the pit. Bottom photo was taken during the later stages of examination after the center of the pit was reached. Mag. 15X.

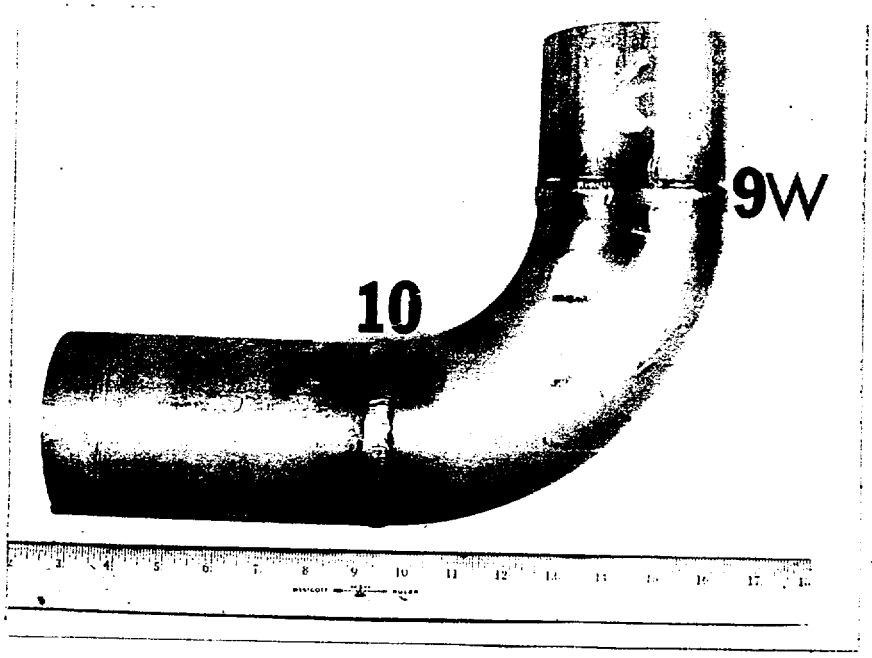

Figure 14: View of the section of pipe containing field weld 9W.

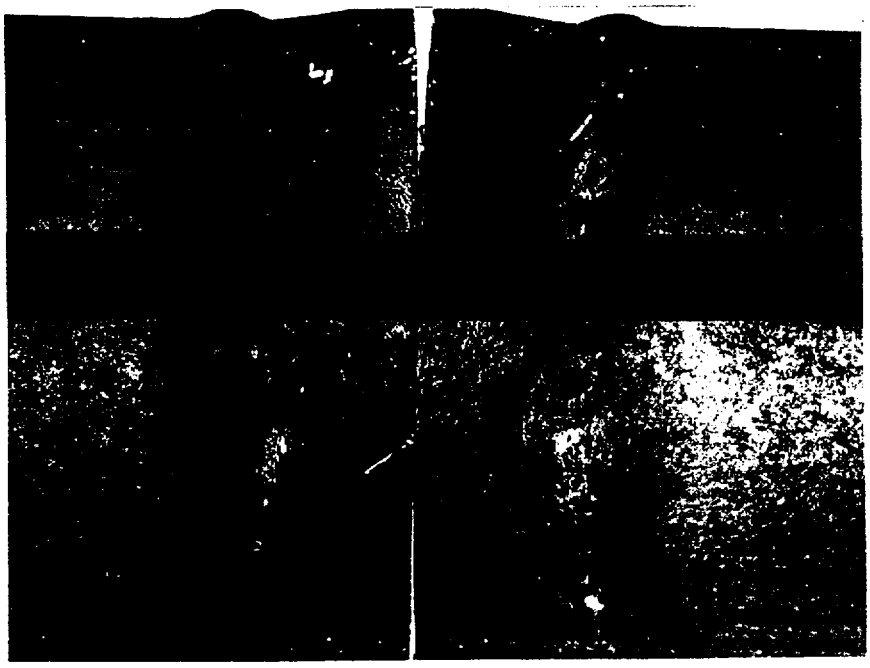

Figure 15: Photograph showing the ID surface of the pipe that contains weld 9W.

Figure 16: Closeup view of the damage (arrow) under the nodule on weld 9W. Mag. 4X.

Figure 17: Photographic montage showing the metallographic cross section taken through the area shown in the previous photo. The pitting at this weld shows extensive branching. Mag. 15X.

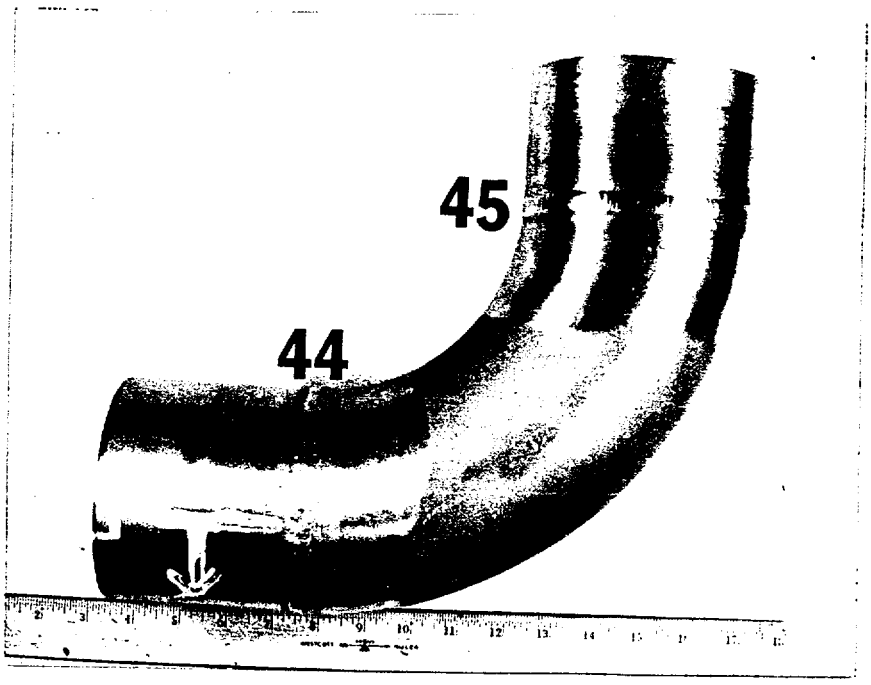

Figure 18: Photograph of the pipe section containing field weld 45.

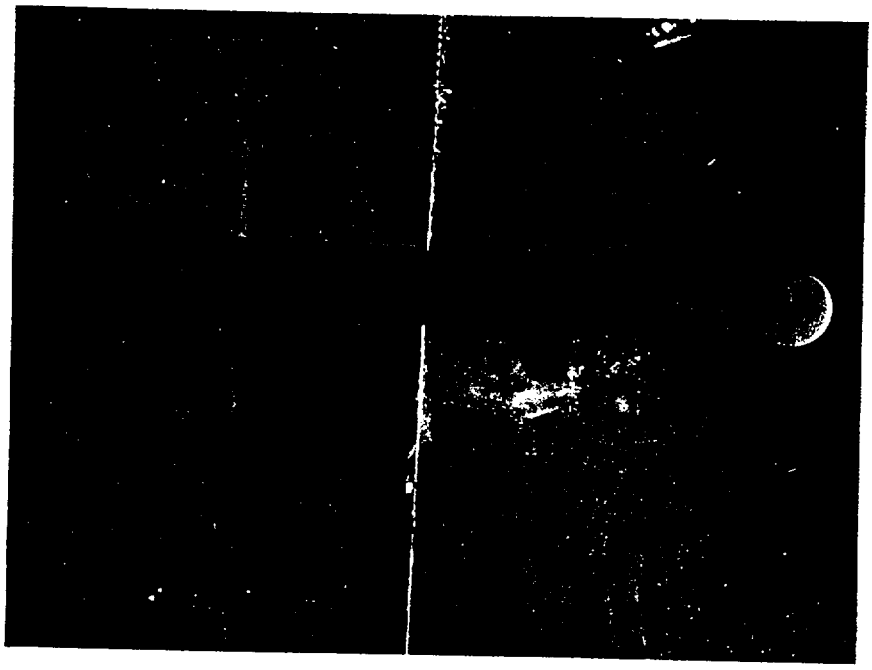

Figure 19: View of the ID surface of weld 45.

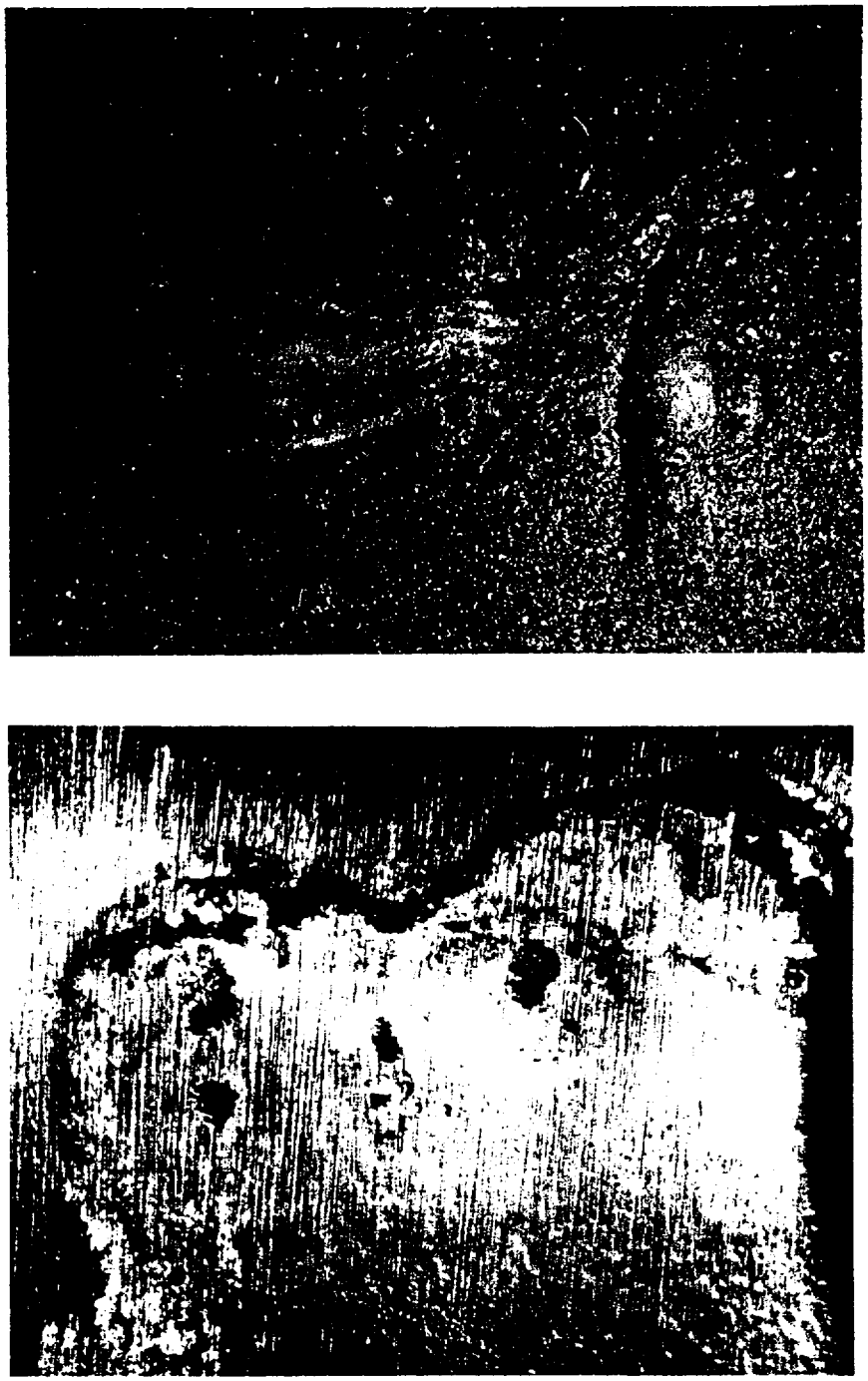

Figure 20: Closeup views of the pitting discovered along the surface of the pipe containing field weld 45. The bottom view was after cleaning of the ID surface. Mag. top- 3x, bottom- 7x.

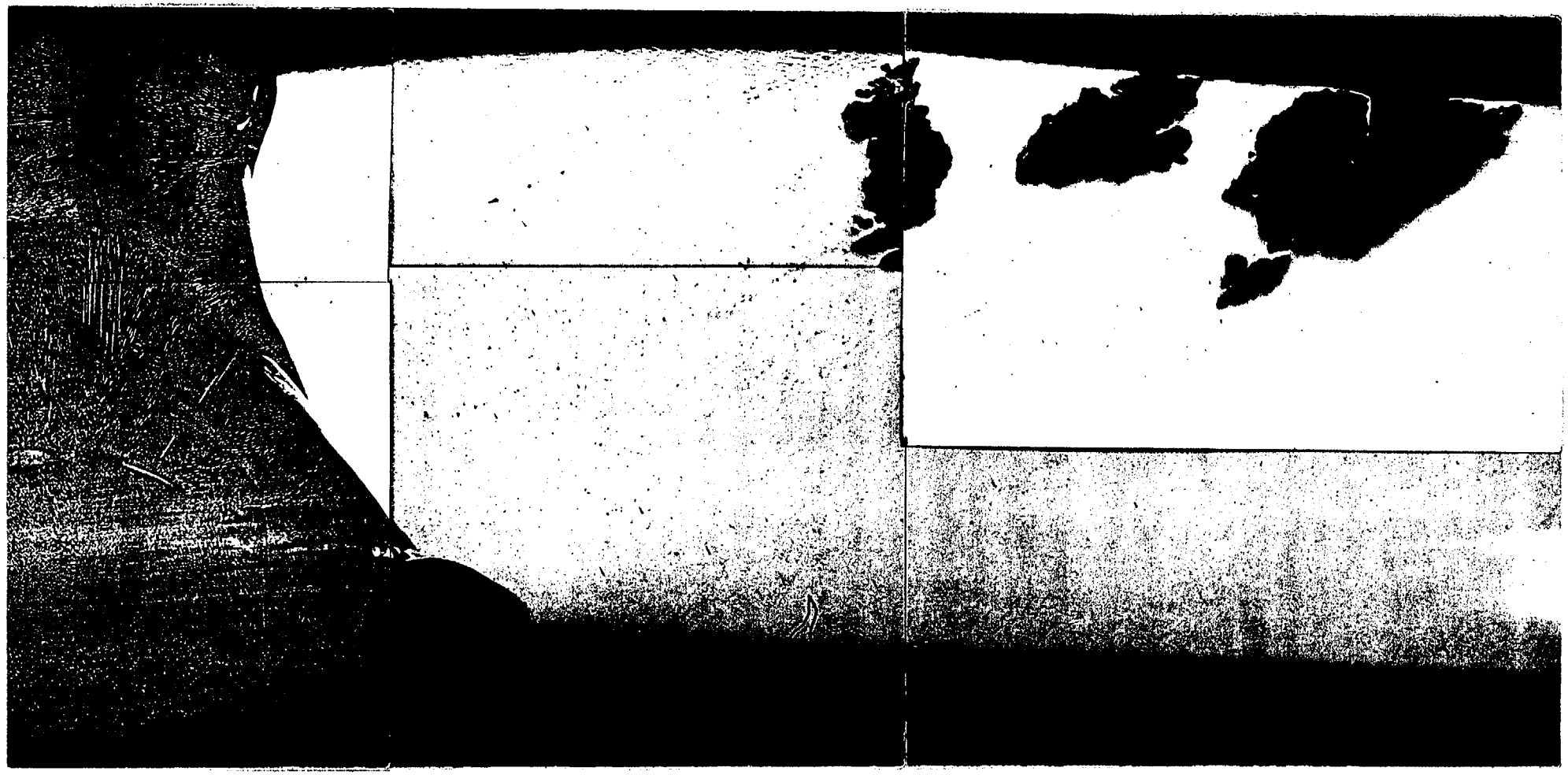

Figure 21: Photographic montage from the metallographic sample prepared through weld 45. The pitting was present only in the stainless pipe and not in the high nickel weld. Mag. 15X.

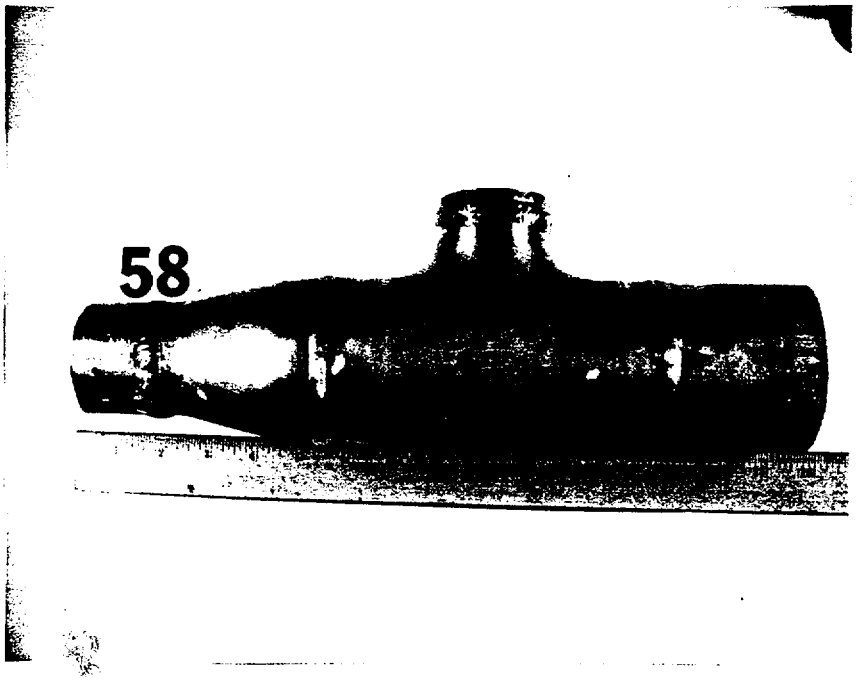

Figure 22: View of the reducer that contained field weld 58.

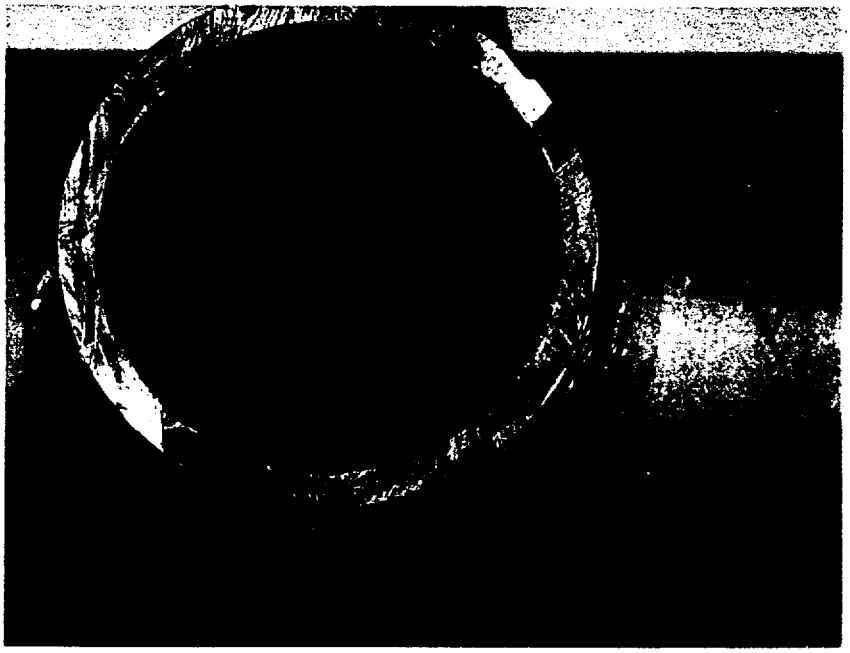

Figure 23: Photograph showing the tubercles along the ID of weld 58.

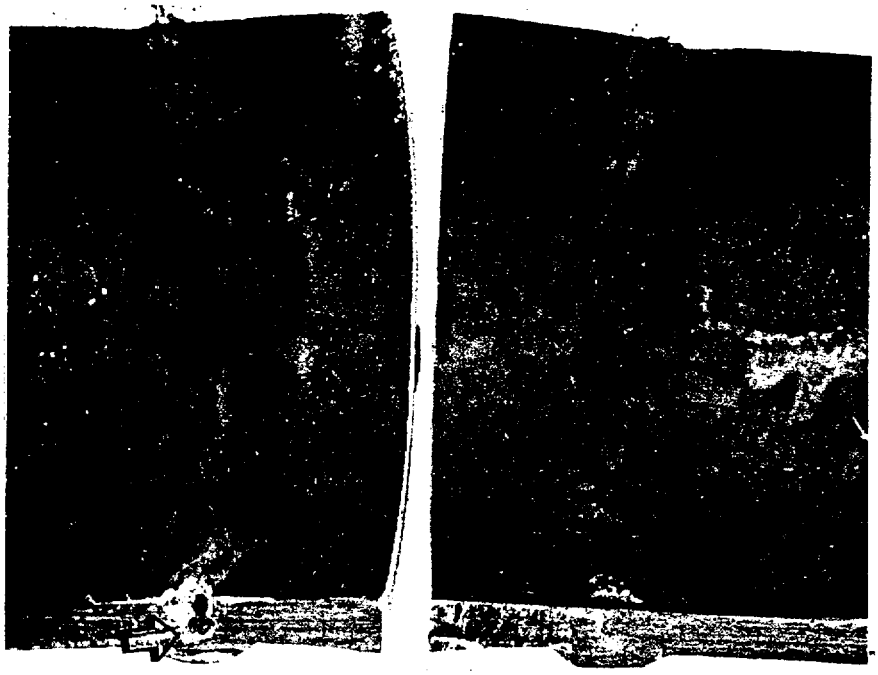

Figure 24: Photograph of the ID surface of the pipe segment containing weld 58 after sectioning. Notice the rough profile of the weld and the evidence of microbial activity by the deposits and staining along the surface. Arrow indicates porosity in the weld that was visible after sectioning the pipe.

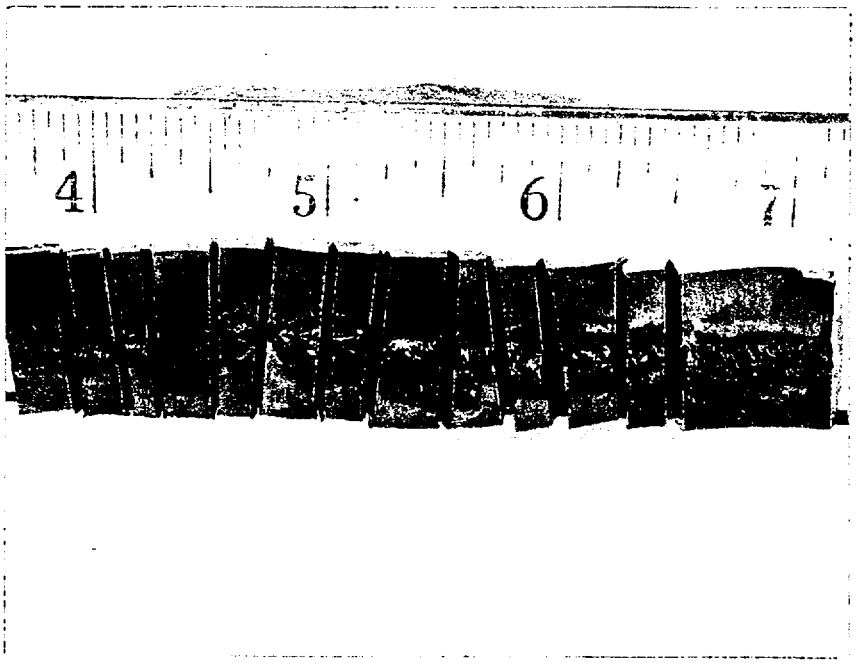

Figure 25: Photograph showing a portion of the weld after cleaning and sectioning approximately every 1/8 of an inch. Notice the very rough appearance of the weld.

Figure 26: Photograph showing several of the cross sections that were taken through weld 58. Notice the cracking and large amount of porosity in several of the sections. Mag. 2X.

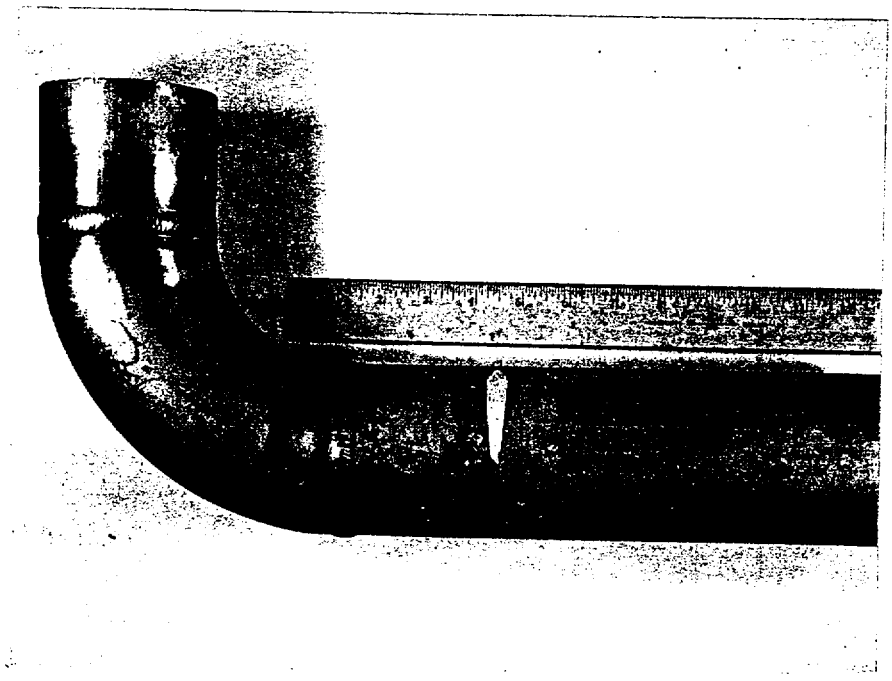

Figure 27: Photograph showing leaking weld 3"-WS-74-163-Q3-FW97 between the straight piece of pipe and the elbow.

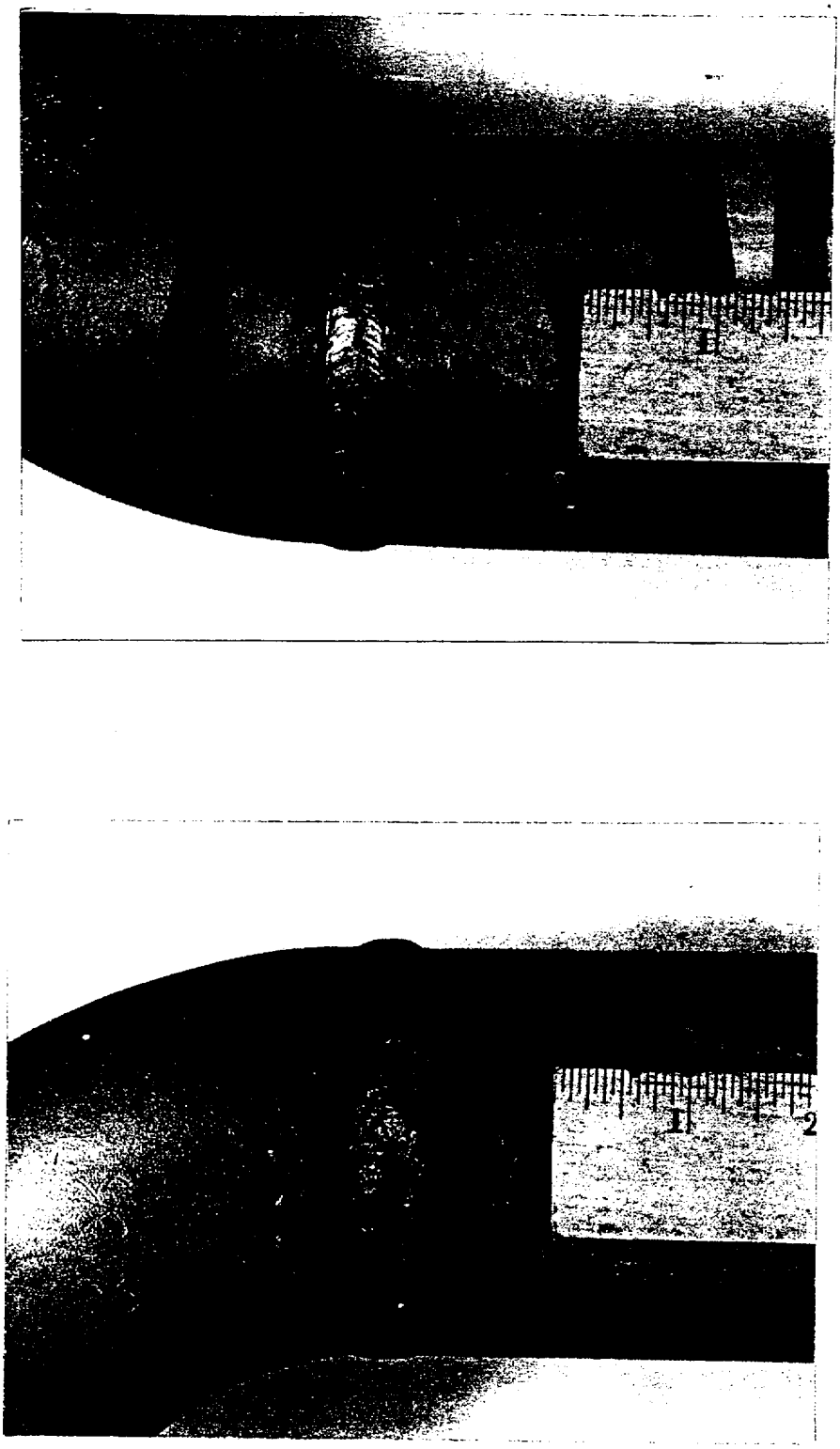

Figure 28: Close-up photographs of two opposite sides of the weld shown in Figure 27. Note the apparent staining on the pipe and weld in the bottom photo and the more irregular appearance of the weld cover pass.

Sample "A"

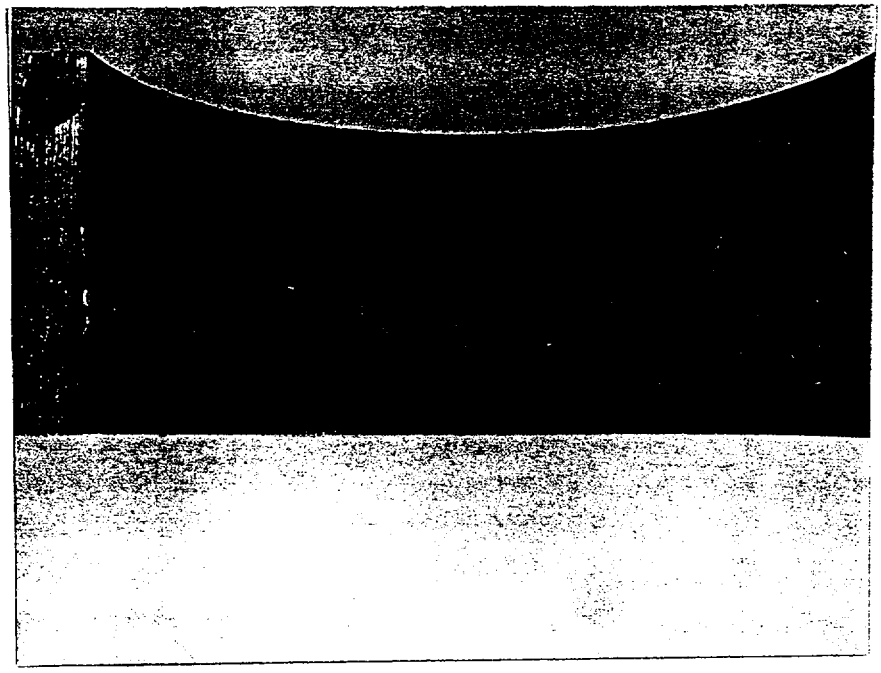

Sample "B"

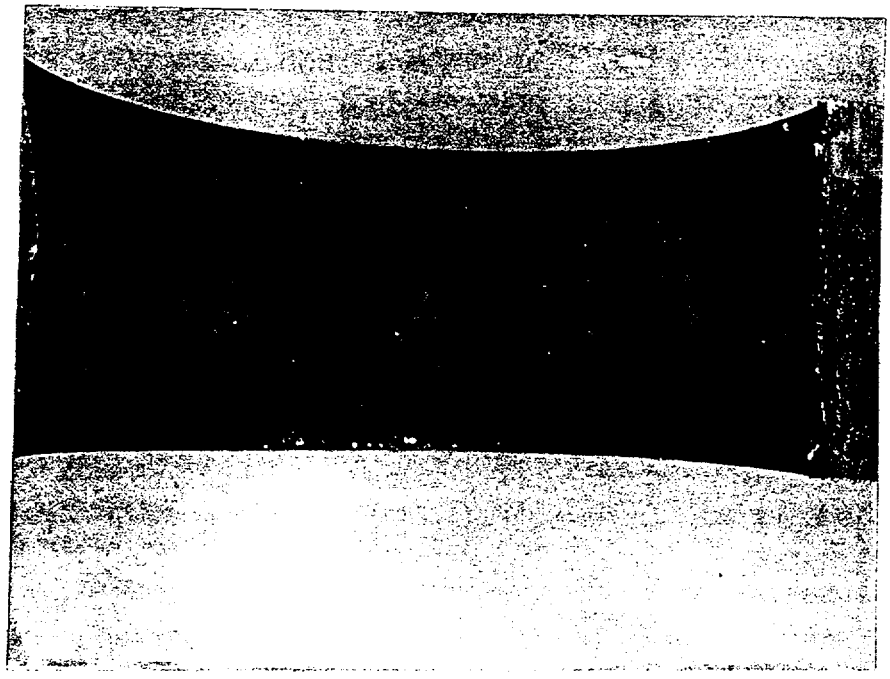

Figure 29: Photographs of opposite halves of the root circumference of FW97 prior to cleaning showing evidence of well developed corrosion nodules typical of the MIC process. The halves are identified as "A" (top) and "B" (bottom) for reference. Magnification about 1.5X.

Sample "A"

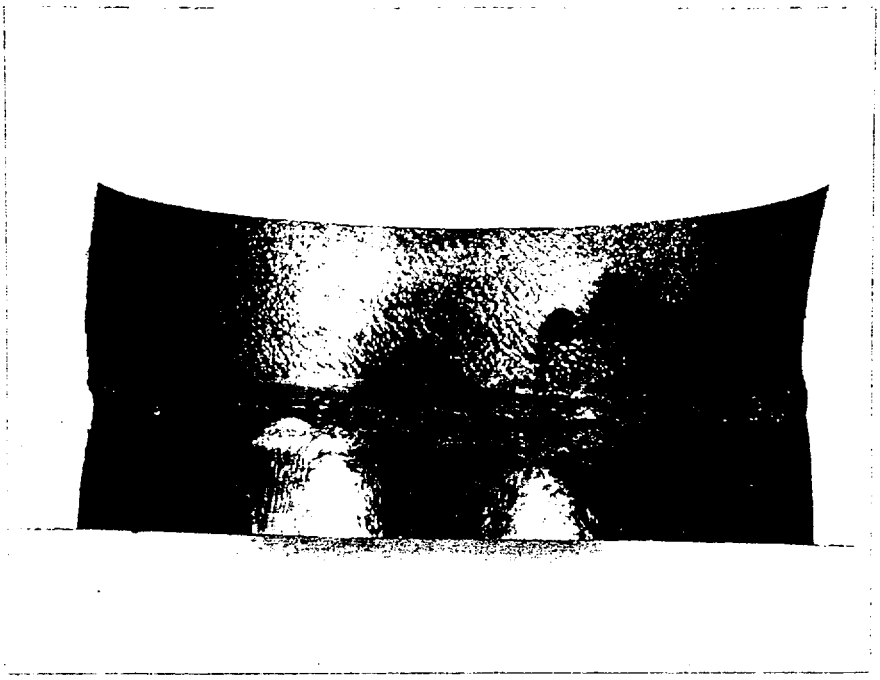

Sample "B"

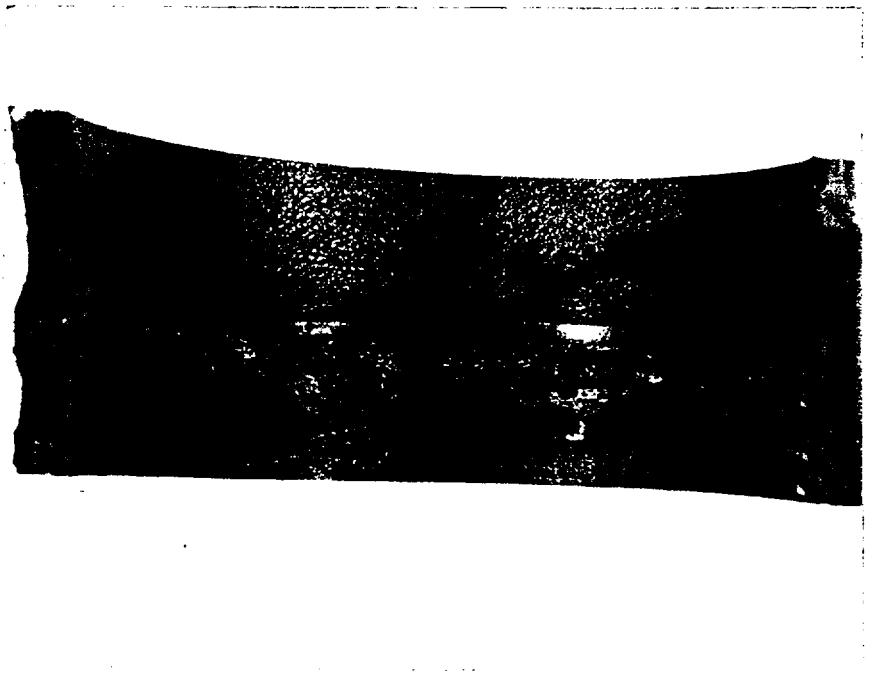

Figure 30: Photographs of the halves of the weld shown in Figure 29 after cleaning. From these it can be seen that there are significant weld root anomalies in addition to the MIC damage. A void associated with the MIC attack, and possibly some lack of fusion, is visible on the left edge of sample Sample "B". Magnification about 1.5X.

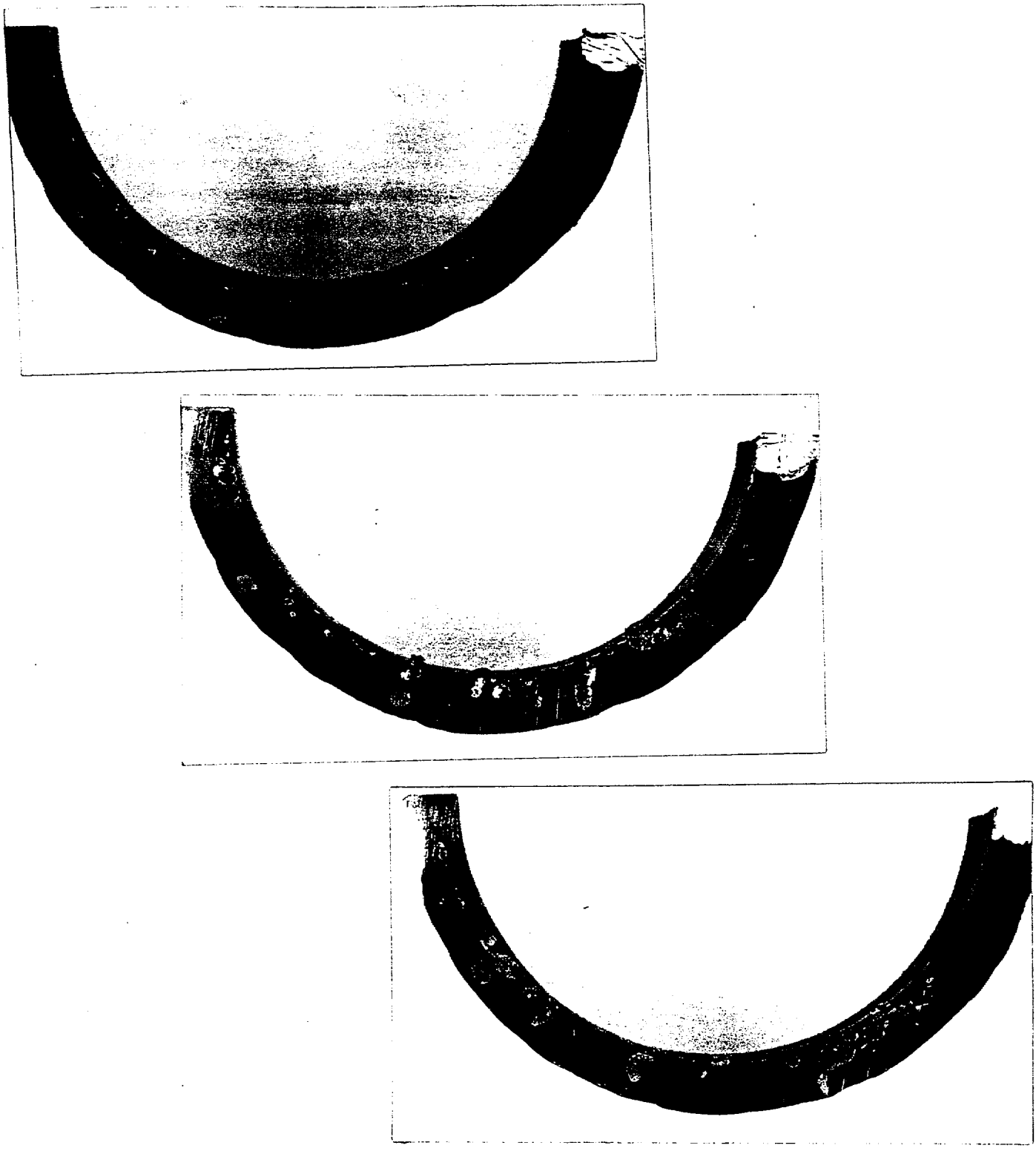

Figure 31: Three photographs showing progressive stages of grinding through FW97 in sample "B". The middle photo is at about the centerline of the weld and the other two are from about 0.080 inches either side of the center line. The extent of the MIC attack is evident. Magnification about 1.5X.

Memorandum

[redacted]

VIRGINIA POWER
NORTH CAROLINA POWER

To: R. L. Rasnic, NAPS
From: L. L. Spain, IN/3NW

Innsbrook Technical Center
February 5, 1997

MATERIALS ENGINEERING LABORATORY REPORT
NESML-O-295A

The attached Materials Analysis Report, NESML-Q-295A, dealing with microbiologically influenced corrosion in stainless steel service water piping, specifically socket (fillet) welded piping, and referrd to in the transmittal memo for report Q-295 is provided for your use.

If you have any questions or comments please do not hesitate to contact me at Innsbrook on 730-2602.

Leslie L. Spain

Attachments

cc: E. W. Throckmorton, IN/3NW
R. V. Shears, NAPS
B. W. Foster, NAPS
S. M. Kotowski, NAPS
M. D. Sartain, NAPS
David Hughes, NAPS
C. E. Sorrell, IN/1NW
R. C. Sturgill, IN/1NW
J. I. Bennetch, IN/3NW
J. G. Beck, IN/GW w/o
Records Management, Materials Analysis Report, NESML-Q-295A

NES MATERIALS ENGINEERING LABORATORY
FAILURE ANALYSIS REPORT
January 31, 1997

NESML-Q-295A

1. Station: North Anna Power Station **2.** Unit: 1 and 2

3. Sample Origin: Various fillet welds from socket welded portions of the service water system.

4. Safety Classification: Safety Related

5. Description of Failure: During walkdowns to look for leaking service water piping several socket welded connections were identified as probable leakers or possibly past leakers. The lab was asked to evaluate about six of the welds which were removed from service.

6. Laboratory Conclusions: The laboratory was unable to confirm any leakage or through wall indications as the result of microbiologically influenced corrosion (MIC), or any other cause. The only indications of any volumetric type flaw found in the material sent to the lab were three small voids located near what was probably FW66 on a 2 inch line. These were not shown to be surface connected on either the inside or outside surface of the pipe. In general, the welds which the lab sectioned for examination were in good condition with little or no indication of welding defects or other type of flaws.

7. Discussion:

Visual Inspection and Light Microscopy: The welds received in the lab were identified only by the weld numbers etched or stamped in the piping next to the welds so the lab was not able to determine the precise location of all of the piping but understands generally it was from the chiller rooms and the charging pump service water piping. Figure 1 shows three of the welds, FW76, FW73, and FW96, and is representative of the balance of the material the lab received. Note that all of the welds were cut at or very near the junction of the pipe with the shoulder of the socket weld fitting to which it was attached. The consequent cuts removed a significant portion of the fillet welds in some cases. The welds and piping were closely examined for signs of leakage such as holes, deep pitting, and rust stains similar to what has been observed in

the past on the service water butt welds. No definitive indications were noted. Suspect locations were identified on field welds 67, 73, 74, 90 and 96. These were sectioned, ground and polished in an effort to identify MIC attack and assess weld condition. Figures 2, 3, 4, 5, and 6, respectively, show representative longitudinal cross sections through these welds with no indications of MIC or other weld anomalies noted. Welds FW73 and FW74 were sectioned and progressively ground transversely to assess weld condition and to isolate any MIC attack. Figures 7 through 13 show successive stages of grinding into these welds in 1 millimeter increments and reveal no anomalies in the welds.

In the course of the lab's efforts an anomaly was noted in the end of the pipe opposite FW67 near marking that indicated the area must have been contiguous to FW66. Figure 14 shows the end of the pipe turned so the field weld marking is visible while Figure 15 is oriented so a rust stain on the pipe surface is visible. Finally, Figure 16 shows the end of the pipe with three small voids in the wall which may represent MIC attack. The rust stain previously noted was on the pipe near the largest of the voids.

EDS Analysis: Analysis of four of the welds, FW67, FW73, FW74, and FW97, by energy dispersive spectroscopy, which is capable of semi-quantitative elemental analysis, produced nearly identical spectra. The spectra indicate the weld filler metal was an austenitic stainless steel weld consumable such as ER308 or ER308L.

8. Conclusions: The lab was unable to find any conclusive evidence of microbiologically influenced corrosion on any of the six welds that were evaluated. The one case in which voids which may have been caused by MIC were found involved base metal attack which may have been at a weld to base metal interface; however, because the weld in question, FW66, was not provided with the pipe and because the voids did not appear to penetrate either the outside or inside wall of the pipe the lab did have, it can not be said conclusively where the MIC started. As a general rule the welds which were sectioned and polished were found to be high quality without any evidence of weld anomalies such as slag, porosity, or lack of fusion. Because of the way the welds were disconnected from the sockets they were welded to, it was not possible to thoroughly assess the quality of the welds relative to root connected anomalies such as incomplete penetration. Never the less, the

welds appeared to be of good quality with no anomalies that might aggravated MIC attack were it to occur. It was noted, however, that the welds appear to have been made with ER308 type filler metal which, while acceptable, is not optimal for resistance to MIC. A filler metal such as ER309MoL or ER316L would be preferred.

9. Recommendations: In the future if socket welded stainless steel service water lines are identified with confirmed weld leaks, the leaking piping should be removed in a way that preserves all of the fillet weld(s) and surrounding base material if at all possible. It is recognized that in some cases this will increase the scope of the repair effort, which may be undesirable, and that assessment of the benefit of optimizing the failure analysis effort will have to be made on a case by case basis.

Prepared by: _____
Leslie L. Spain

Reviewed by: _____
J. G. Beck

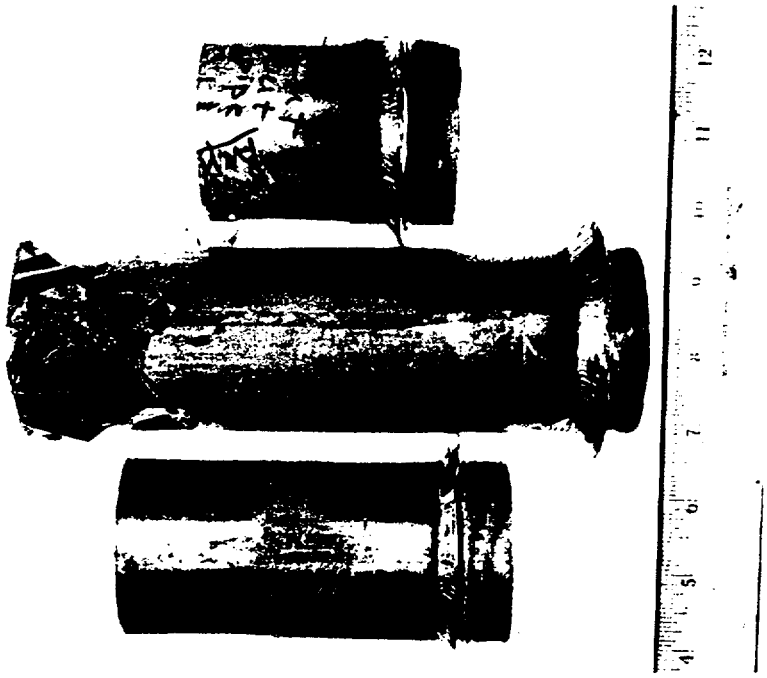

Figure 1: Photograph of welds FW73 (top), FW96 (middle), FW67 (bottom) showing the as received condition of the welds with some staining thought to indicate leakage locations.

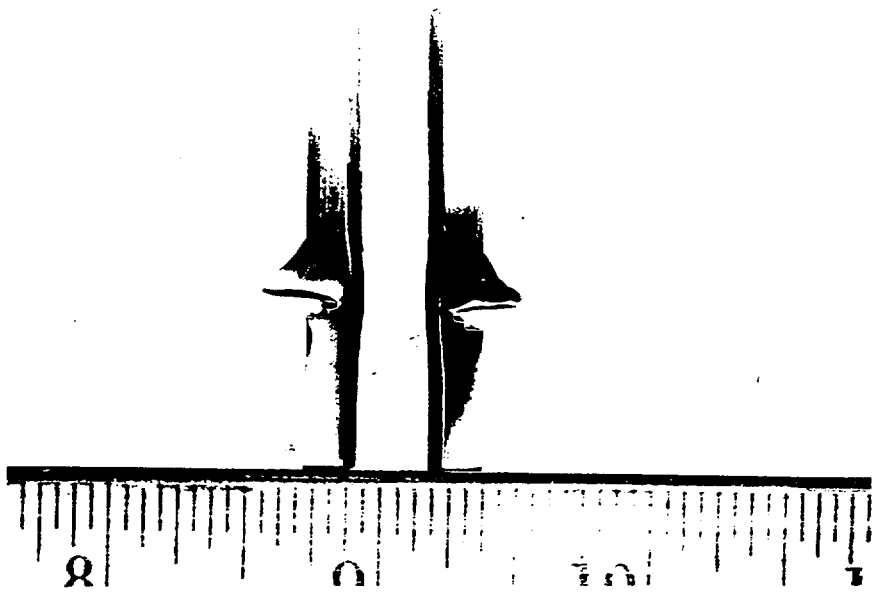

Figure 2: Photograph of a potential leak location identified on FW67. No evidence of MIC attack or weld anomaly is evident.

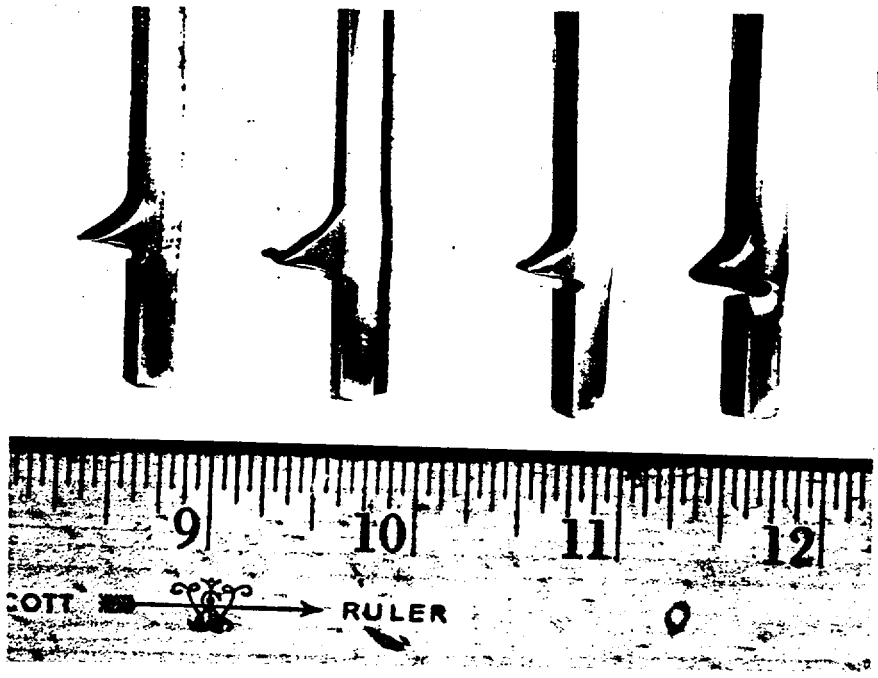

Figure 3: Photograph of four sections of FW73 cut and polished to assess weld condition and identify MIC. No questionable looking areas are apparent.

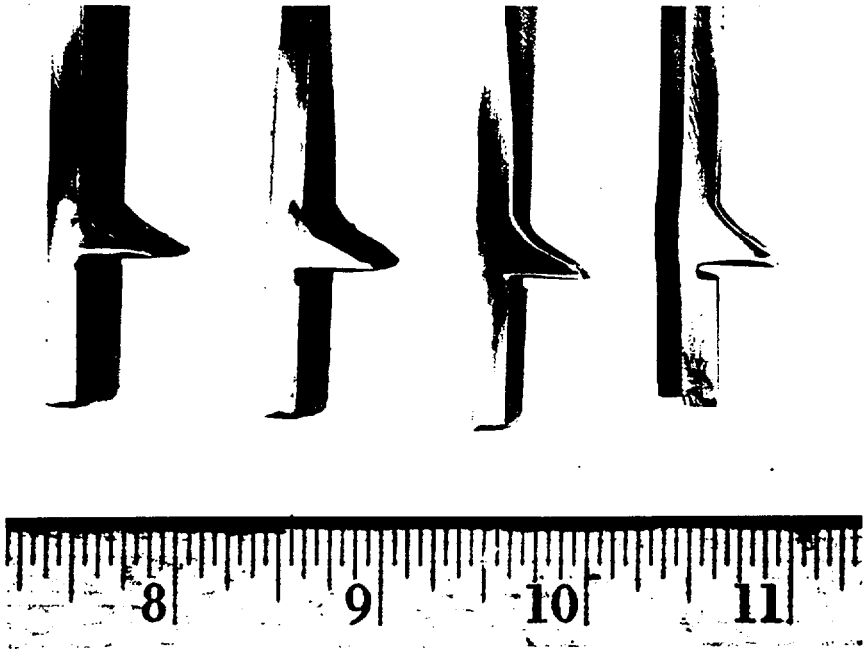

Figure 4: Photograph of four sections of FW74 prepared to show weld quality and locate MIC attack. No weld defects or MIC were found.

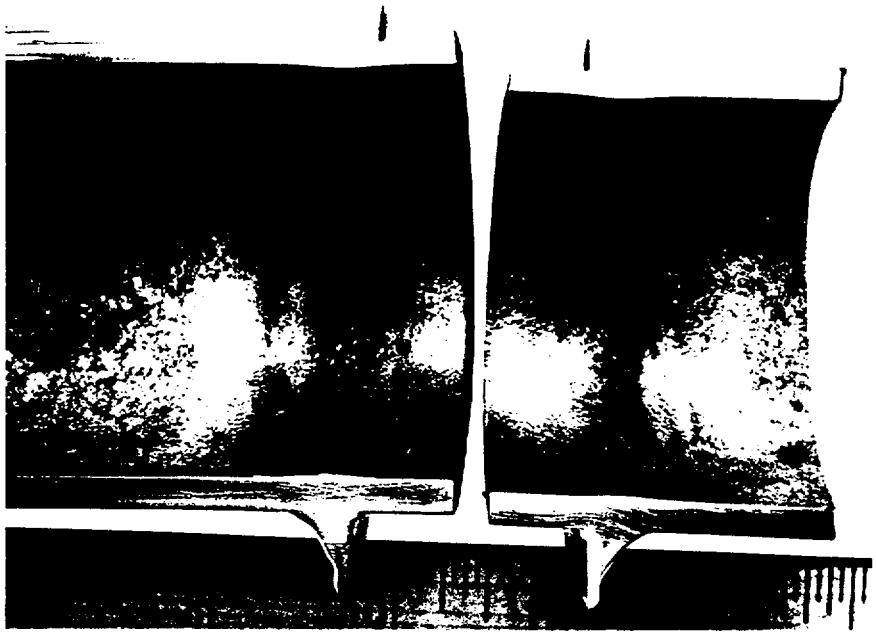

Figure 5: Photograph of a cross section of FW90 showing sound weld with no flaws or apparent MIC attack.

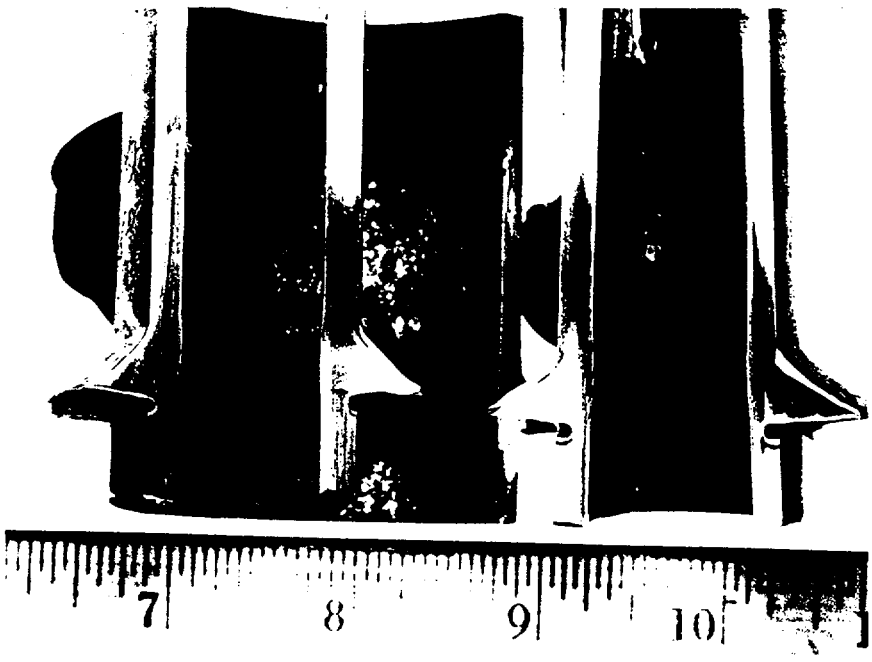

Figure 6: Photograph of four cross sections through suspected leak locations on FW96. No MIC indication or other weld anomalies were found.

Figures 7 - 13: The following series of Figures is photographs of successive stages of grinding in approximately 1 millimeter increments through FW74 (left) and FW73 (right) from what remained of the root of the welds to their toes. No anomalous indications of any type were noted.

Figure 7: At remaining weld root.

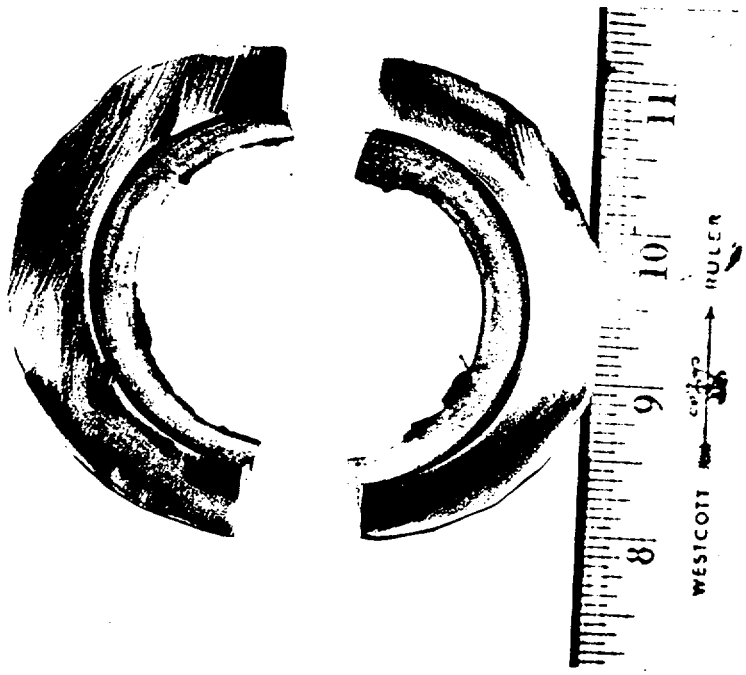

Figure 8: About 1.0mm into welds.

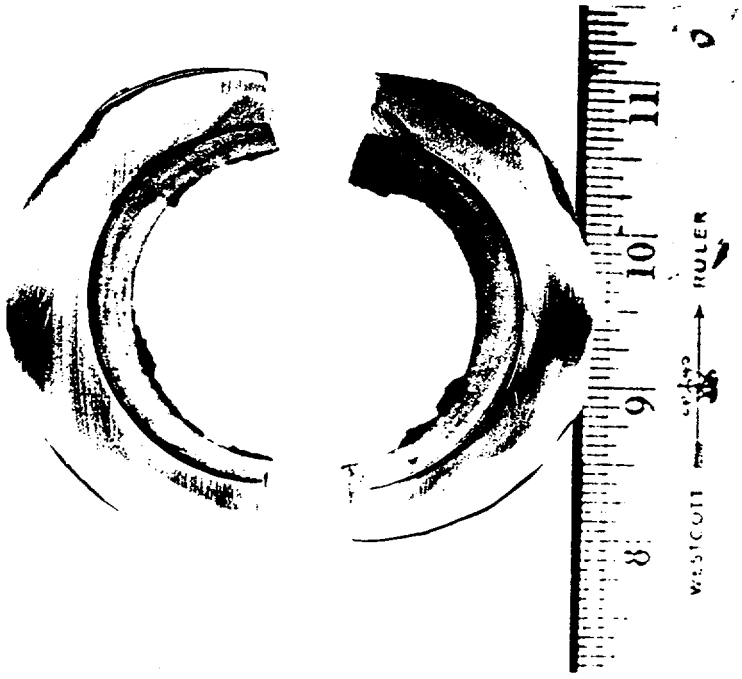

Figure 9: About 2.0mm into the welds.

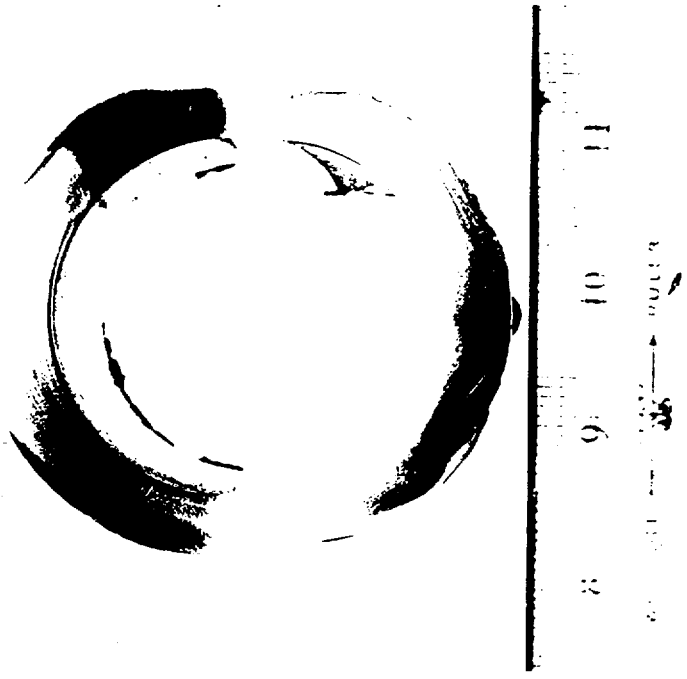

Figure 10: About 3.0mm into the welds.

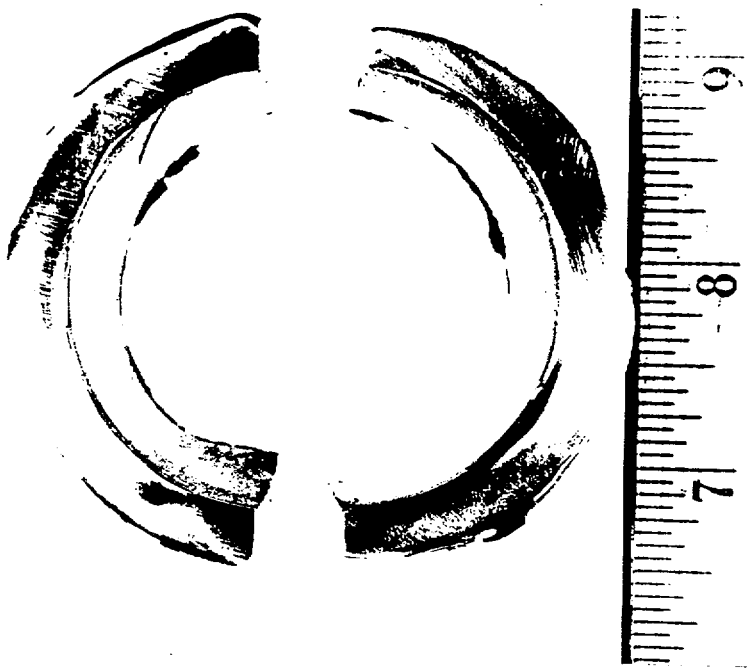

Figure 11: About 4.0mm into the welds.

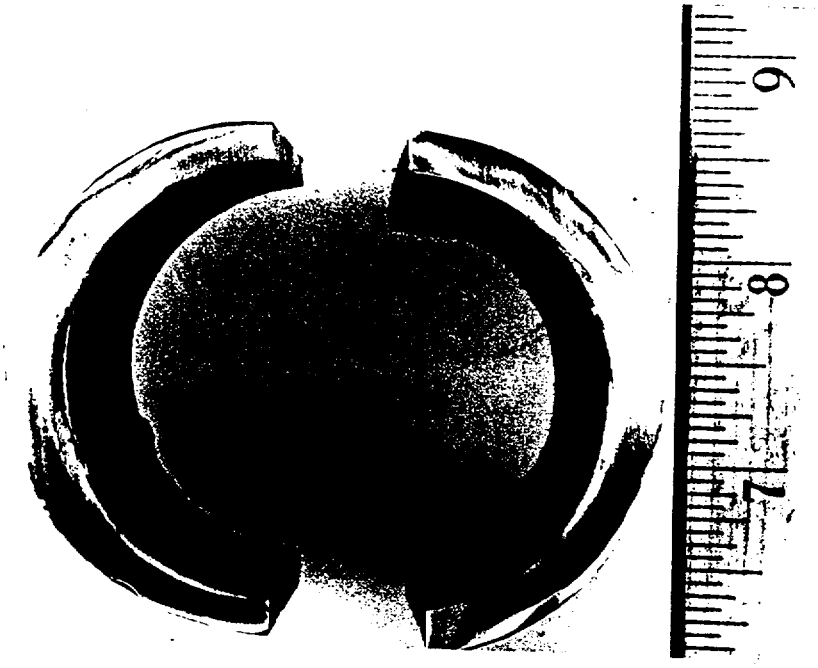

Figure 12: About 5.0mm into the welds.

Figure 13: At the toe of the fillet welds after about 6.0mm of grinding.

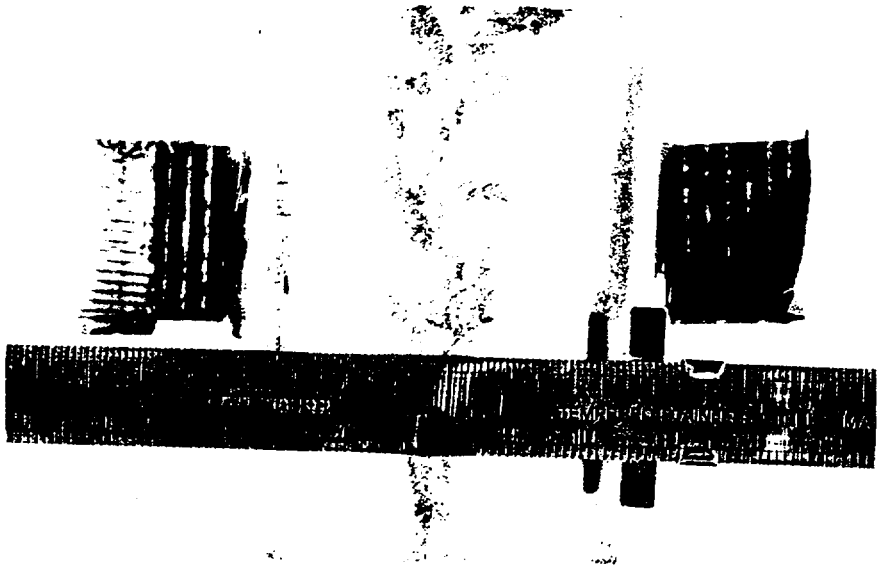

Figure 14: Photograph of the end of a piece of pipe marked FW66 opposite the end where FW67 was found and presumed to be contiguous to FW66.

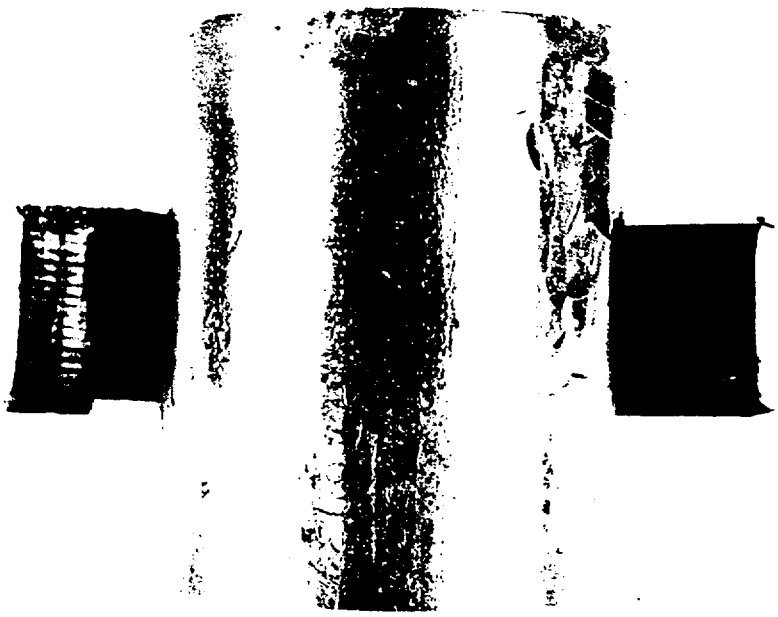

Figure 15: Photograph of the section of pipe in Figure 14 turned to show the rust stain on the outside surface

Figure 16: Photograph of the end of the pipe shown in the preceding two figures. Three small voids are visible in the wall of the pipe which may indicate MIC attack.

Memorandum

[redacted]

VIRGINIA POWER
NORTH CAROLINA POWER

To: David Hughes, NAPS
From: L. L. Spain, IN/3NW

Innsbrook Technical Center
August 6, 1997

MATERIALS ENGINEERING LABORATORY REPORT
NESML-Q-322

The attached Materials Analysis Report, NESML-Q-322, concerning two leaks in service water system piping, is provided for your use. If you have any questions or comments please do not hesitate to contact me at Innsbrook on 730-2602.

Leslie L. Spain

Attachments

cc: E. W. Throckmorton, IN/3NW
R. V. Shears, NAPS
B. W. Foster, NAPS
S. M. Kotowski, NAPS
R. L. Rasnic, NAPS
J. G. Beck, IN/GW w/o
Records Management, Materials Analysis Report, NESML-Q-322, INGW

NES MATERIALS ENGINEERING LABORATORY
FAILURE ANALYSIS REPORT
July 31, 1997

NESML-Q-322

1. **Station:** North Anna Power Station 2. Unit: 2

3. **Sample Origin:** The pipe submitted to the lab was associated with a fillet weld designated 9W on line 2"-WS-84-163-Q3 and a butt weld designated 19W on line 3"-WS-75-163-Q3. It was reported that weld 19W was made with Inconel filler material approximately 6 months prior to the failure.

4. **Safety Classification:** Safety Related

5. **Description of Failure:** The leaks, which were discovered during routine walk down of the service water system, both appeared to be located adjacent to the OD toes of the affected welds.

6. **Laboratory Conclusions:** Both leaks appear to be the result of microbiologically influenced corrosion that began in heat tinted base material on the ID of the pipe. In the case of the fillet weld (9W) the MIC pitting grew to the heat affected zone (HAZ) of the weld and then proceeded along the HAZ, with some weld metal attack, and perforated the pipe at the pipe side weld toe at the HAZ/fusion line. The butt weld attack was confined entirely to base material with no apparent attack of weld metal or HAZ.

7. **Discussion:**

Visual Inspection and Light Microscopy:

9W - The section of piping containing weld 9W as received in the lab and after sectioning is shown in Figures 1 through 5. Figure 1 is an overview of the 2 inch pipe to reducing coupling showing the staining on the pipe, weld, and coupling indicative of leakage. The suspected leak location at the toe of the fillet weld is indicated by an arrow and is shown at higher magnification in Figure 2. A section through the pipe and coupling showing the leak location is shown in Figures 3, and 4. Figures 3 shows the ID leak location after sectioning and prior to removal of the accumulation of corrosion product and debris. Figure 4 shows the same area at higher magnification after cleaning. The suspected initiation location for the MIC pitting that led to the leak is indicated by the arrow. Finally, Figure 5 is a composite photograph showing the area at higher magnification with evidence of significant additional pitting. Just discernible from these photographs is the fact that all of the pitting had started on the ID pipe wall under the fillet weld

in base material which had been slightly discolored or "blued" by the heat of the welding process.

19W - Field weld 19W was a butt weld between a 3 inch schedule 163 stainless steel pipe and a 3"x2" reducer. The weld was reported to have been made with Inconel filler material. Figure 6 is a photograph of a cross section through the reducer, weld, and pipe showing both halves of the section. A large, rounded, rust colored nodule can be seen just to the side of the weld ID root in an area of the pipe base metal that appears to be slightly discolored, "blued", from the welding heat. Figure 7 shows a close up of the same area after removal of the nodule with the suspected leak initiation site indicated by an arrow. Figure 8 is a view on the OD of the pipe showing the suspected leak location which is indicated by the arrow. Given the magnification of the photograph, the indication is about 2 millimeters (.080") from the OD toe of the weld.

Metallography:

9W - Cross sections were cut through the pipe and fitting in attempt to locate the ID pit initiation location and the point of OD penetration, and to assess the extent of the pit growth. Figures 9 through 13 illustrate these successive stages of grinding. Figure 9 clearly shows the OD location where the MIC pit formed. Figures 10, 11, and 12 show progressive growth of the pit through the pipe material. Of particular interest is the fact that when the pit reached the weld/base metal interface it began to follow the HAZ of the weld while attacking the weld metal itself to a lesser extent. During progressive grinding of the specimen shown in Figure 12, the OD penetration point was discovered at the toe of the weld. Unfortunately, further sample preparation ground past the hole and back into sound metal resulting in the sample shown in Figure 13. The ligament of material between the pit and the OD surface of the pipe at this point is about .002 inches thick.

In addition to the cross sections discussed above, cross sections were prepared that show the root of the fillet weld and the general microstructure of weld and base metal. Figures 14 through 18 illustrate these cross sections. Figure 14 is a composite that shows the entire weld cross section. Of particular interest in the figure is the large number of individual passes (estimated at 15 to 20) that comprise the weld. Normally in a fillet weld of this size one would expect to see 3 to 5 passes. Figures 15 an 16 are successive close ups of the root of the weld which appear to show a small amount of corrosive attack into the weld metal at the root. Figures 17 and 18 are successive views which illustrate a tendency for some

differential etching of the bulk of the weld metal, the base metal, and the weld metal in the fusion zone. This may be related to the excessive heat input associated with the unusually large number of passes in the weld.

19W - Cross sections through weld 19W were prepared to determine the leak location and to assess microstructural detail. Figure 19 shows the first of the cross sections exhibiting two voids associated with MIC pitting adjacent to the weld and near perforation at both the OD base metal surface (top of sample) and the ID surface (bottom of sample). The next progressive cross section is shown in Figure 20 at a higher magnification. It shows enlargement of the larger of the previous voids with penetration at the OD surface and progression toward the ID surface. Figure 21 is a composite photograph that shows the pit penetration at the ID surface. In all of these figures it can be seen that the pitting does not appear to affect weld metal or HAZ but rather is confined to base metal.

EDS Analysis:

9W - The base metals and weld metal associated with weld 9W were analyzed by energy dispersive spectroscopy (EDS), which is capable of elemental identification and semi-quantitative constitutional analysis. In all three cases the spectral traces and analyses were consistent with expected results for AISI type 316L, or 316, stainless steel which was the identified material type for the piping and weld.

19W - The base metals and weld metal associated with weld 19W were analyzed by energy dispersive spectroscopy (EDS), which is capable of elemental identification and semi-quantitative constitutional analysis. The spectral traces and analyses for the pipe and reducer were consistent with expected results for AISI type 316L, or 316, stainless steel which was the identified material type. Analysis of the weld metal revealed analyses and spectral traces consistent with as deposited filler metal meeting the composition requirements of specification SFA 5.14, types ERNiCr-3, ERNiCrFe-5, or ERNiCrFe-6, any one of which may have been used to weld field weld 19W.

In addition to analyses of the base metals and weld metal of weld 19W it was possible to perform analyses of the large nodule and other corrosion product/scale recovered form the inside of the pipe. These analyses revealed some areas with unexpectedly high levels of manganese, sulfur, and chlorine. These elements are often found in conjunction with microbiologically influenced corrosion type pitting.

8. Conclusions: Both leaks investigated by the lab were probably the result of microbiologically influenced corrosion. The pitting morphologies were typical of MIC attack, particularly by the bacteria Gallionella. These bacteria are known to concentrate iron, manganese, and chlorine which were found in chemical analyses of the corrosion products associated with weld 19W. In both cases the attack appears to have started adjacent to the welds in the zone of material that had been discolored by welding heat but not in the microstructurally evident heat affected zones. In the case of the fillet weld, 9W, attack eventually involved the actual weld HAZ and some attack of weld metal. No involvement of weld metal or HAZ was noted with the leakage at weld 19W which was made with an Inconel type filler metal.

It was reported that weld 9W was made about 7 years ago while weld 19W was made approximately only 6 months ago. It must be recognized that neither of the resulting time spans to leakage is inconsistent with the potential of MIC damage. Such factors as the efficacy of biological control measures, cleanliness of the piping and water, piping surface condition, etc., can have significant effect on the time to initiate pitting. Once pitting has started, the environmental conditions created by the colony of bacteria in the pit can be extremely aggressive. Through wall perforation may happen quite quickly after pitting begins or may take a relatively long time. With the variabilities in the time to initate pits and the pit growth rate, the time to perforation may vary considerably from one situation to another.

Prepared by: _____
Leslie L. Spain

Checked by: _____
J. G. Beck

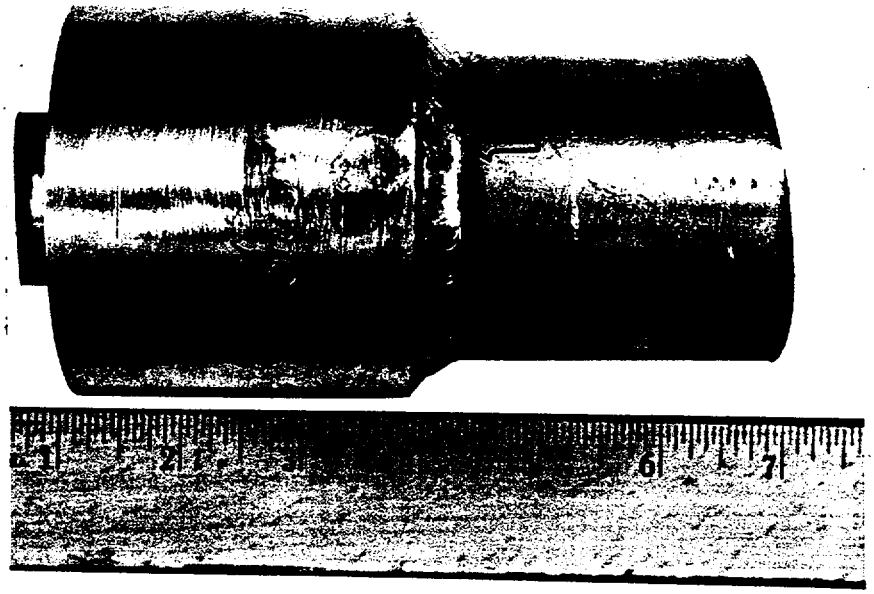

Figure 1: As received view of the reducer and pipe at field weld 9W of line 2"-WS-84-163-Q3. Rust colored staining is evident on the weld and fitting. The apparent source of leakage is indicated by the arrow.

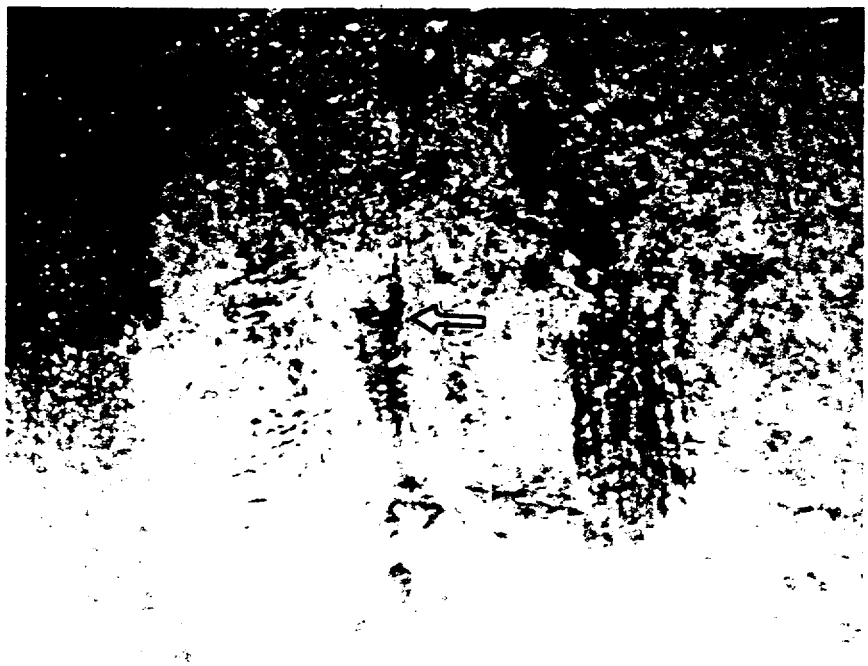

Figure 2: A photograph at weld 9W showing the apparent leak location, indicated by the arrow, adjacent to the pipe side toe of the weld. Magnification about 25X.

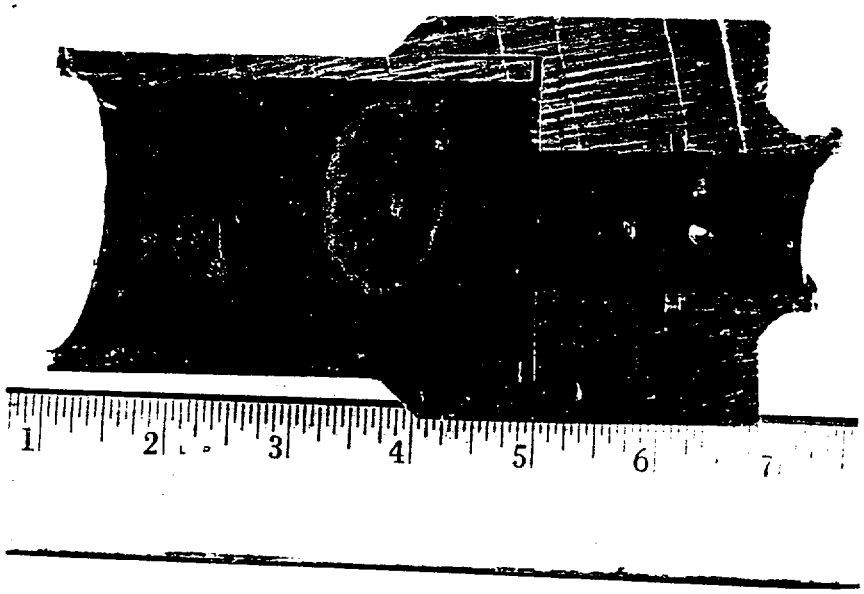

Figure 3: Photograph of a cross section through the pipe and fitting at weld 9W. The build up of debris and corrosion product is evident. The lighter orange spot in the large light orange area is the suspected leak initiation location.

Figure 4: A higher magnification photograph of the cross section shown in Figure 3 after removal of debris and corrosion product. The apparent leak initiation is indicated by the arrow but other ID pitting is evident. Magnification about 1.5X.

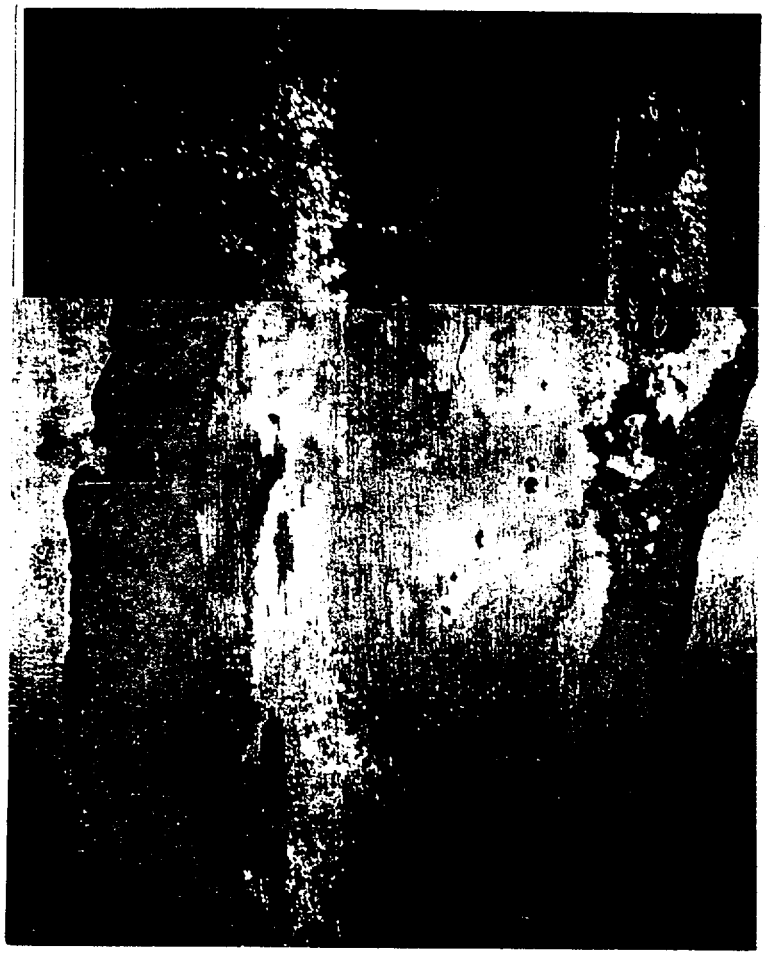

Figure 5: Photographic montage of the pitting shown in Figure 4 at still higher magnification showing its extent and relative size. The pitting spans the "blued" region under the fillet weld on the pipe ID. Magnification about 3X.

Figure 8: Photograph showing the pipe OD at the leak location. The suspected site of leakage is at the arrow to the left of the OD weld toe. Magnification about 5X.

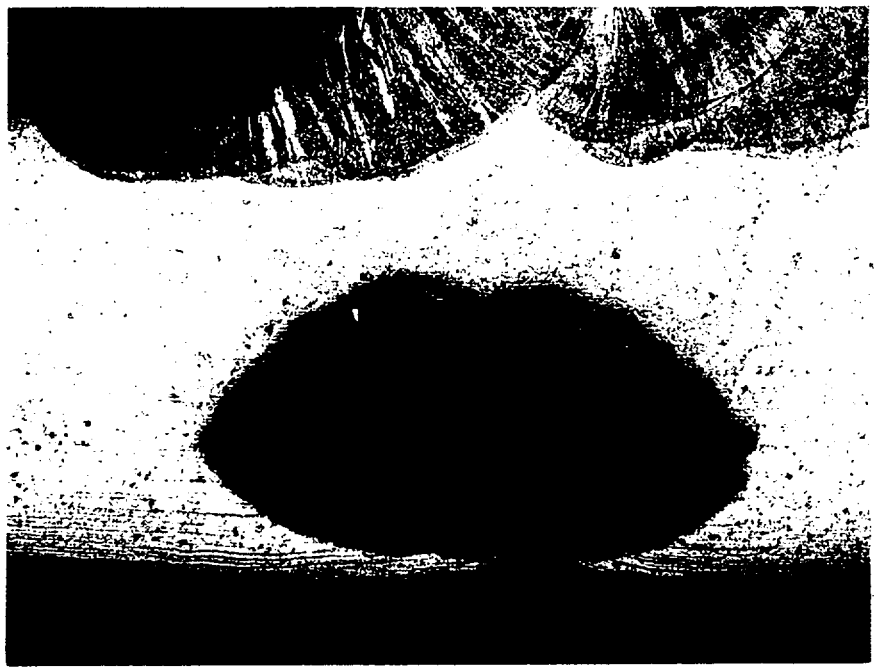

Figure 9: Photomicrograph of a cross section through the pipe and fillet weld at weld 9W. The small size of the pit at the ID surface relative the cavity size is evident and typical of some forms of MIC attack. This is the first of a series of cross sections at the suspected leak location. Magnification 15X. Electrolytic oxalic acid etch.

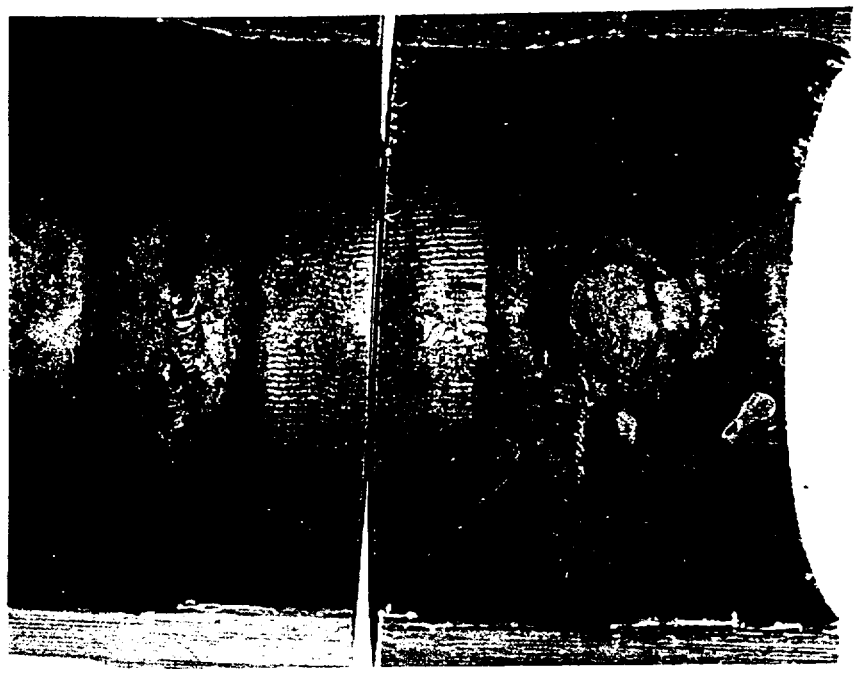

Figure 6: Photograph of the cross section through the reducer and pipe at field weld 19W on line 3"-WS-75-163-Q3 showing a well developed nodule just to the right of the ID weld toe on the "blued" material of the pipe. Magnification about 1X.

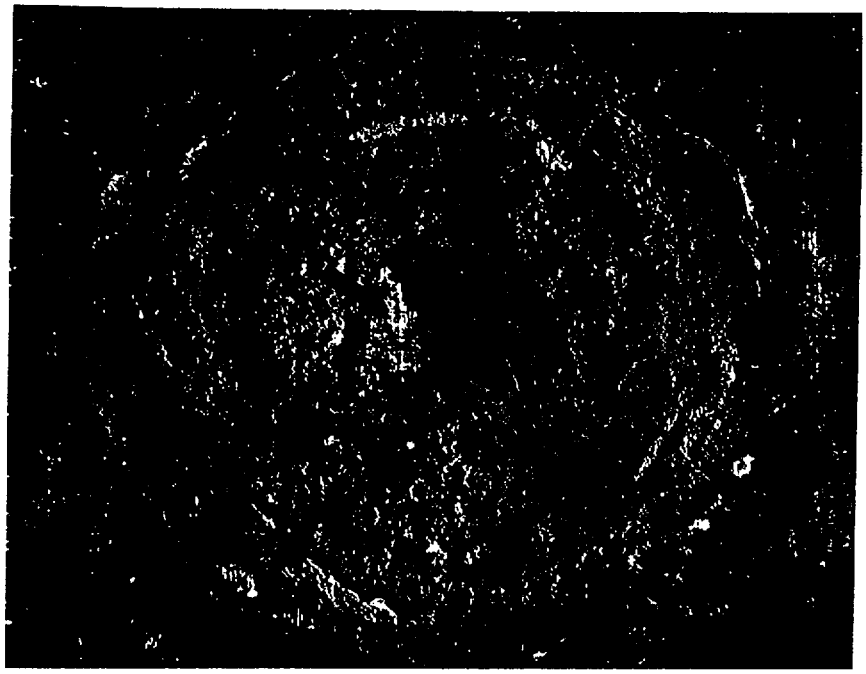

Figure 7: Higher magnification of the area under the nodule shown in Figure 6. The suspected MIC pit is at the arrow. Magnification about 5X.

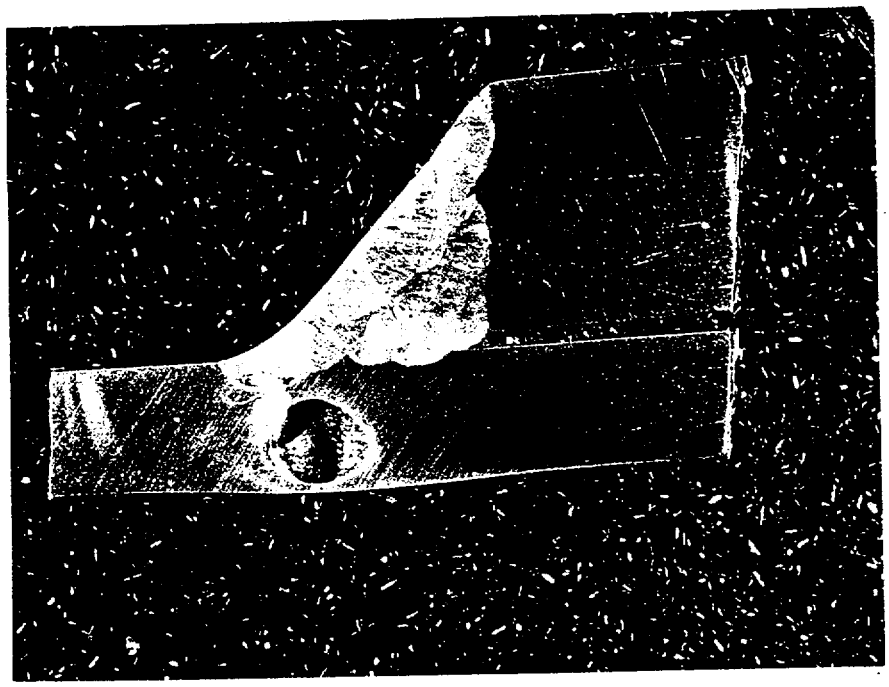

Figure 10: Photograph of the second of the series of cross sections at weld 9W. The larger size of the cavity and its encroachment on the fillet weld HAZ are evident. Magnification about 4X. Electrolytic oxalic acid etch.

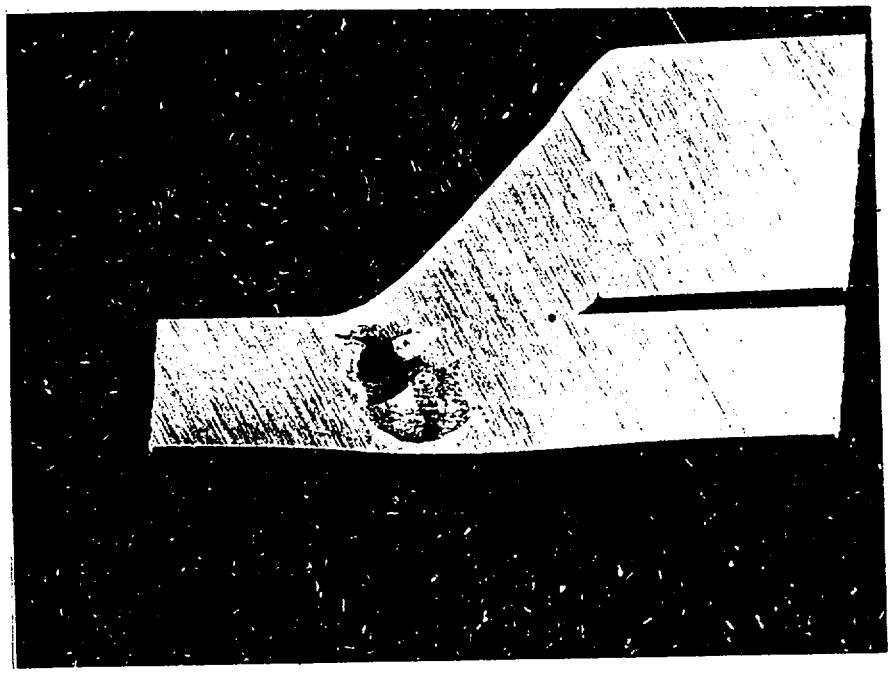

Figure 11: The next in the series of weld 9W cross sections showing the extensive cavity associated with the leak, preferential growth along the weld HAZ, and some weld metal attack. Magnification about 4X.

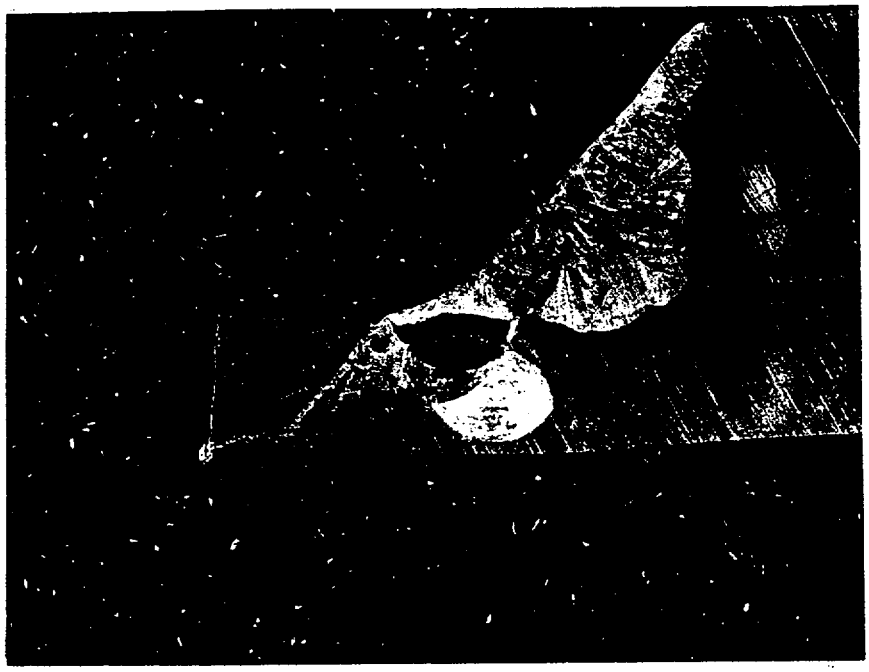

Figure 12: Another in the series of cross sections showing the extent of the cavity and attack along the HAZ and in the weld metal just before the point where the cavity broke through the OD surface at the weld toe. Magnification about 4X. Electrolytic oxalic acid etch.

Figure 13: Photomicrograph of the final cross section of the series at the leak location just past the point where the penetration of the OD surface was found, but unfortunately, not photographed. The preferential attack along the HAZ is clearly indicated here, Magnification 100X. Electrolytic oxalic acid etch.

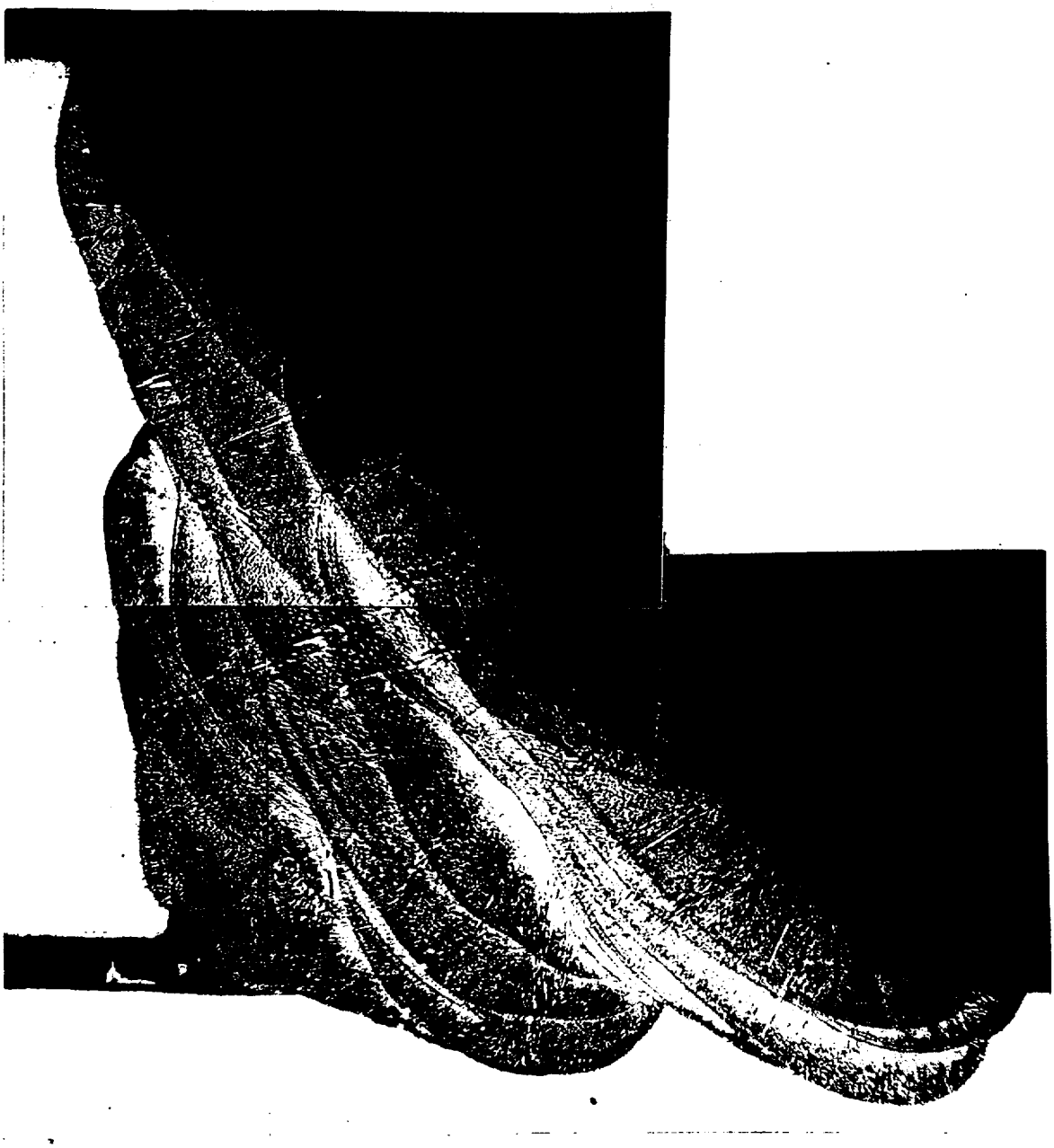

Figure 14: Photomicrographic montage of a cross section through weld 9W showing the structure of the weld and indicating an unusually large number of weld passes. Magnification 15X. Electrolytic oxalic acid etch.

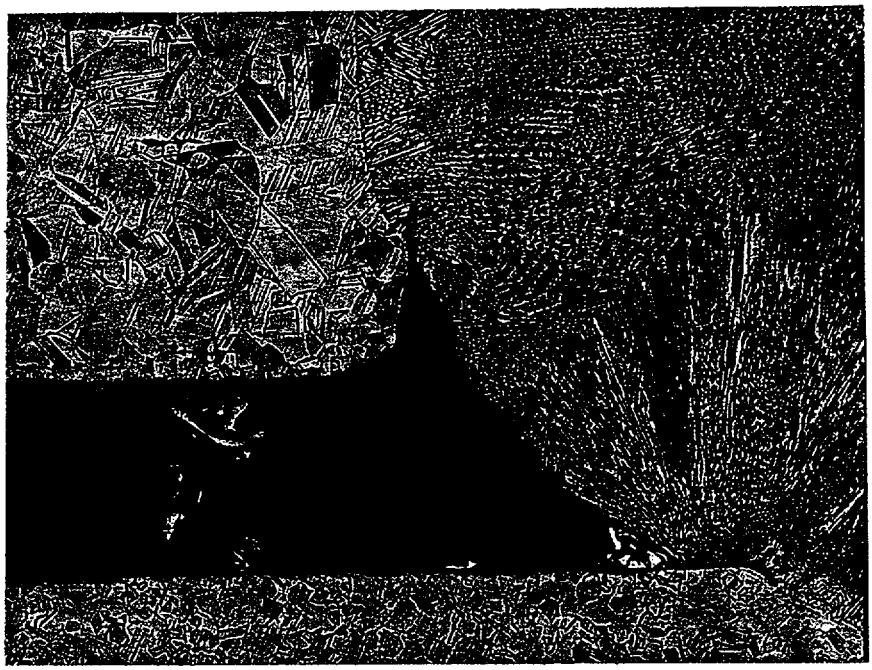

Figure 15: A higher magnification photomicrograph of the root of weld 9W. The base metal and weld metal microstructures are evident and appear normal in this view. Note the incipient attack of weld metal at the root tie in points. Magnification 50X. Electrolytic oxalic acid etch.

Figure 16: Photomicrograph showing the incipient attack of the weld metal at the root of weld 9W. Magnification 200X. Electrolytic oxalic acid etch.

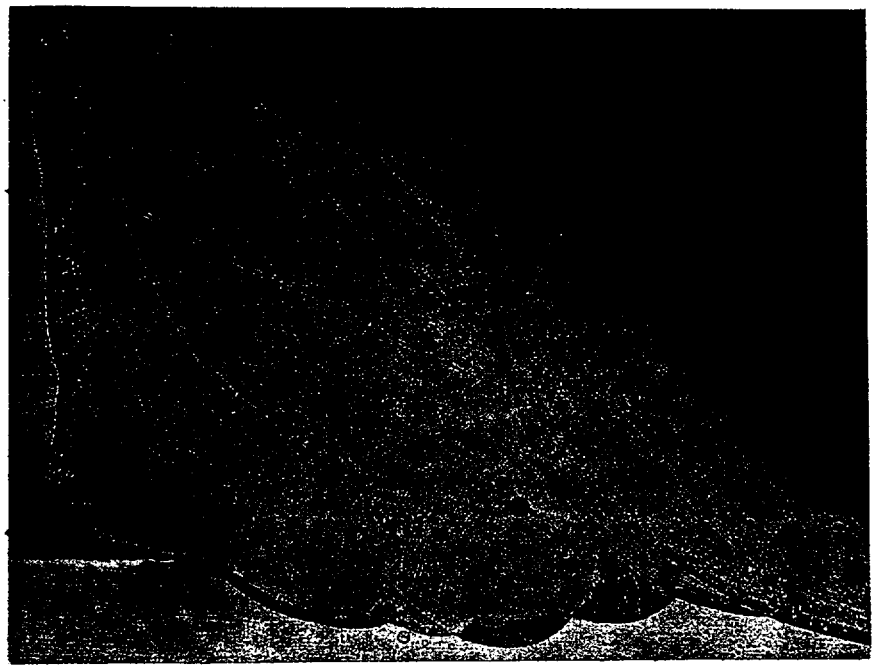

Figure 17: A photomicrograph of weld 9W that shows the tendency for certain portions of the weld to etch differently than the bulk of the weld or the base material. This may be related to excessive heat input from the large number of weld passes. Magnification 15X. Electrolytic oxalic acid etch.

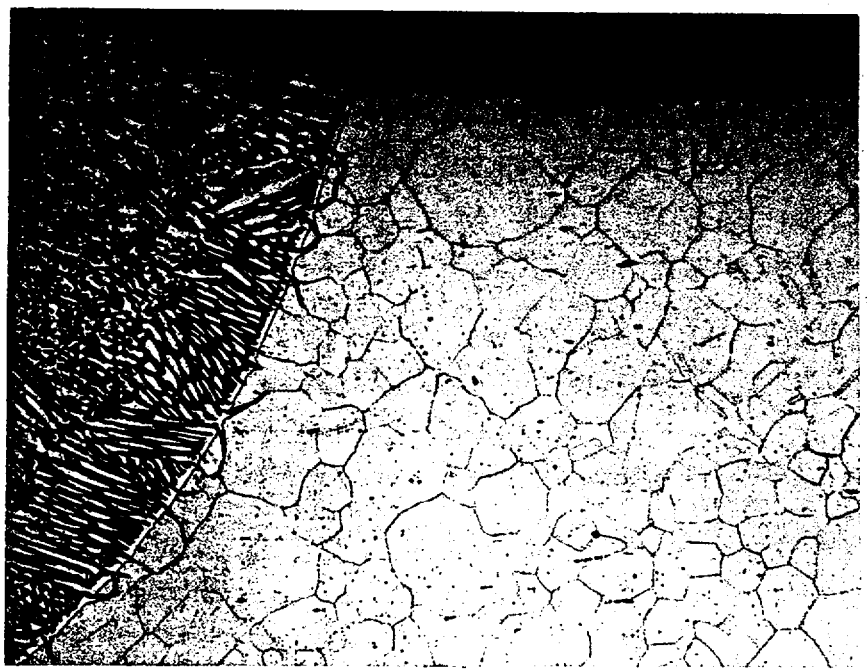

Figure 18: A higher magnification photomicrograph at the weld HAZ of 9W showing the heavy etching of the weld metal indicating an enhanced susceptibility to corrosion. Magnification 200X. Electrolytic oxalic acid etch.

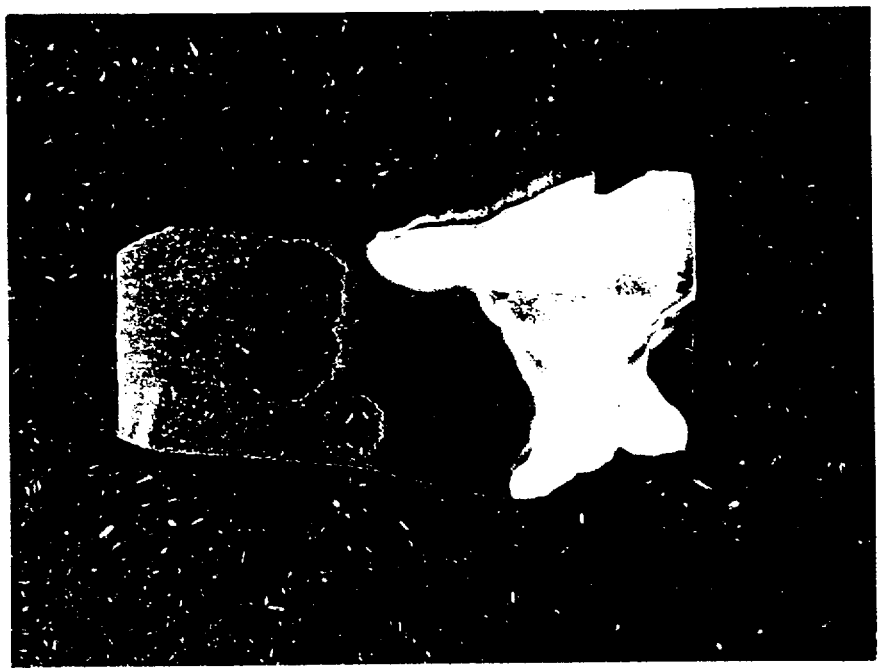

Figure 19: Photograph of a cross section through the leak location of weld 19W showing the large subsurface cavity compared to the small perforation at the OD surface. No involvement of weld or HAZ is indicated. Magnification about 5X. Electrolytic oxalic acid etch.

Figure 20: Photomicrographic montage of the second in a series of cross sections at weld 19W again showing the large cavity compared to the exit point on the OD surface. Magnification 15X. Electrolytic oxalic acid etch.

Figure 21: Photomicrographic montage of the last in the series of cross sections at weld 19W showing the ID entrance to the cavity and showing no involvement of weld or HAZ. Magnification 15X. Kallings etch.